Document No.: TR-02-005.1

Document Title: Thermochronological Evolution of Calcite Formation at the Proposed Yucca Mountain Repository Site, Nevada: Part 1, Secondary Mineral Paragenesis and Geochemistry

Document Revision: 0

Originators: Nicholas S. F. Wilson and Jean S. Cline; Department of Geoscience, University of Nevada Las Vegas, 4505 Maryland Parkway, Box 454010, Las Vegas, Nevada, USA 89154-4010

PI (Jean S. Cline) signature: Jean S. Cline

Date: 5/20/02

QA Manager (Amy Smiechiski) signature: Amy J. Smiechiski

Date: 5/20/02

Technical Reviewer: Robert Bodnar, Virginia Tech, Blacksburg, Virginia

Technical Reviewer signature: Robert J. Bodnar

Date: 05/16/2002

Table of Contents

Table of Abbreviations

BZ barren zone
CAZ calcite alteration zone
CL cathodoluminescence
DOE Department of Energy
DPTS doubly polished thick sections
ECRB Enhanced Characterization of the Repository Block Cross Drift
EPMA electron probe microanalyses
ESF Exploratory Studies Facility
IFZ intensely fractured zone
LA-ICP-MS ablation inductively coupled plasma mass spectrometry
LC lithophysal cavities
LCZ lithophysal cavity zone
MGSC magnesium-enriched growth-zoned sparry calcite
NPR north portal and ramp
PMC patchy Mg-enriched calcite
PTn Paintbrush Tuff nonwelded
SPR south portal and ramp
SZ saturated zone
UCCSN University and Community College System of Southern Nevada
USGS United States Geological Survey
UZ unsaturated zone
WDS wavelength dispersive spectrometry

Abstract

In the near future a decision will be made as to whether or not Yucca Mountain, 90 miles northwest of Las Vegas, Nevada is a suitable site for a permanent, underground, high level nuclear waste repository. A major factor in determining the suitability of Yucca Mountain as a repository is the potential for the site to be flooded by water during the regulatory lifetime. The current study was undertaken to examine the past fluid history at the site, to gain a better understanding of the possibility of flooding in the near geologic future. To estimate the past fluid flux into the repository horizon, research has focused on secondary minerals that precipitated in open space in lithophysal cavities, fractures, and breccias in the host Miocene tuffs. U.S. Geological Survey researchers concluded that secondary minerals formed from descending surficial meteoric fluids in a vadose environment. State of Nevada scientists observed 2-phase fluid inclusions with homogenization temperatures of 35 to 85 °C in secondary minerals and concluded that these minerals formed in the phreatic environment from upwelling hydrothermal fluids. They further concluded that upwelling hydrothermal fluids repeatedly invaded the site, have invaded the site in the recent geologic past, and could do so again making Yucca Mountain an unsafe site for high level nuclear waste storage. These studies did not constrain the timing of incursion of the fluids with elevated temperatures or the extent of this fluid flux across the site.

This report provides the geologic context for subsequent fluid inclusion and geochronological studies (Wilson et al., 2002) that identified the temperature and extent of the fluid incursion and placed absolute temporal constraints on the fluid history at Yucca Mountain. Here we describe a detailed paragenetic study that determined the depositional history of secondary minerals at Yucca Mountain.

One hundred and fifty-five samples of secondary minerals were collected from lithophysal cavities, fractures, and breccias at Yucca Mountain. Extensive petrography, paragenetic studies, and microprobe mapping indicate that early secondary minerals were heterogeneously distributed across the site and consist of variable amounts of calcite, opal, chalcedony, fluorite, and quartz. Early calcite contained variable trace amounts of Mg (up to 1.3 wt. %). Intermediate minerals consist of mainly calcite, often in bladed habits, with minor opal, and chalcedony and quartz. These minerals contain no diagnostic trace element variations. The latest secondary minerals deposited across the site consist of sparry calcite and minor intergrown opal. This sparry calcite exhibits fine (~ 50 μm) Mg-enriched and depleted growth zones and is chemically distinct from all other calcite. Mg-enriched growth-zoned sparry calcite (MGSC) contains up to ~ 1.0 wt. % Mg and has been identified in > 65 % of the samples collected from across the site. MGSC and associated opal are always the paragenetically youngest minerals; where MGSC is not present, young secondary minerals did not precipitate.

Calcite exhibits ranges for $\delta^{13}C$ from -8.5 ‰ to 9.5 ‰, and for $\delta^{18}O$ from 5.2 ‰ to 22.1 ‰. Samples exhibit generally consistent trends of decreasing C and increasing O isotopic compositions from paragenetically older to younger calcite. C and O isotope signatures for MGSC are between 16 ‰ and 20 ‰ for $\delta^{18}O$ and -3 ‰ and -8.5 ‰ for $\delta^{13}C$. However, signatures for the various stages are not unique and are not diagnostic in correlating secondary mineral stages across the site.

Early calcite is generally more luminescent than later calcite, but luminescence was not sufficiently consistent to aid in constraining the paragenetic sequence. LA-ICP-MS analyses indicate that higher levels of U, Th, and Sr are locally present in MGSC compared to paragenetically early calcite, however, this variation is not present in all samples.

An important observation is that 90% of primary and secondary open space in the tuffs at Yucca Mountain contains no secondary mineral record. Where secondary minerals are present, the older secondary mineral record is heterogeneous across the site. However, MGSC, which forms the youngest part of the secondary mineral record, is present in a majority of samples and exhibits a more homogeneous distribution across the site.

Secondary mineral abundances and textures indicate that secondary minerals precipitated in a vadose environment. The observed features are not consistent with secondary mineral precipitation in a phreatic environment saturated with aqueous fluids. Growth zoning in the outermost MGSC is consistent with formation from discontinuous influx of small fluid volumes with variable Mg content from surficial fluids that percolated downwards. Fluctuations in the Mg content in MGSC may be related to climate changes that occurred in the last few million years.

1. INTRODUCTION

Yucca Mountain, Nevada is currently the only site being studied by the U.S. Department of Energy (DOE) as a potential high-level nuclear waste repository (U.S. Department of Energy, 1988). The Yucca Mountain site is unique among repository sites owing to its location, underground, above a deep water table (Winograd, 1981). A major goal of this study was to ascertain whether the deep water table is a stable feature with a lengthy geologic history, or whether fluctuations in water table elevation occurred in the recent geologic past. Such fluctuations would indicate an increased potential for fluctuations during the regulatory lifetime of the repository and would adversely affect the integrity of the site.

To assist in assessing the long-term stability of the site, research has focused on examining secondary minerals that precipitated in primary and secondary pore spaces in the host tuffs. Since secondary minerals formed from fluids that invaded the repository rocks, the secondary minerals have been examined to determine whether they formed in a vadose or phreatic environment, and from downward percolating meteoric fluids or from upwelling hydrothermal fluids.

Previous research on the origin of secondary minerals from lithophysal cavities (LC), breccias, and fractures has led to much controversy. Scientists from the U.S. Geological Survey (USGS) concur that calcite precipitated from downward percolating cold meteoric fluids in a vadose environment (e.g. Paces et al., 1996; 1997; Whelan et al., in press). However, Dublyansky (1998) and Dublyansky et al. (1998; 2001), representing the State of Nevada, reported the presence of two-phase, aqueous fluid inclusions in calcite. They interpreted these fluid inclusions to have trapped upwelling hydrothermal fluids in a system analogous to epithermal mineral deposits, with mineral precipitation occurring in a phreatic environment.

This study focused on determining the origin and timing of precipitation of secondary minerals at Yucca Mountain. In this paper we report results of integrated studies on the petrography of the secondary minerals, electron probe microanalyses (EPMA), cathodoluminescence (CL), laser ablation inductively coupled plasma mass spectrometry (LA-ICP-MS), and C and O stable isotopes to construct a paragenetic sequence for secondary minerals. These paragenetic relationships provided the geologic context for fluid inclusion and geochronological analyses that constrained the absolute temperature and timing of formation of the secondary minerals (Wilson et al., 2002).

2. GEOLOGIC SETTING

Yucca Mountain is located 90 miles northwest of Las Vegas at the western edge of the Nevada Test Site. The mountain is within the Miocene southwest Nevada volcanic field (Christiansen et al, 1977) and the south-central part of the Basin and Range province. Yucca Mountain was initially chosen for study as a waste repository site because of its arid climate with less than 25 cm of rain per year (U.S. DOE, 1988), and the presence of a deep unsaturated zone (UZ) with a water table 400 – 600 m below the present day surface (Winograd, 1981).

Yucca Mountain is a north trending fault block ridge composed of a 1 – 3 km thick sequence of felsic welded and non-welded volcanic tuffs of the Paintbrush Group (Sawyer et al. 1994), and is bounded on either side by alluvial basins (Fig. 1). The Paintbrush Group is

comprised of the Topopah Spring, Pah Canyon, Yucca Mountain, and Tiva Canyon Tuffs, which dip gently to the east at less than 10 °.

The Topopah Spring Tuff, dated at 12.8 Ma, directly overlies bedded rhyolite tuffs of the Calico Hills Formation (Sawyer et al., 1994) and is about 380 m thick in the vicinity of Yucca Mountain (Stuckless and Dudley, in press). In turn the thin Pah Canyon and Yucca Mountain Tuffs overlie the Topopah Spring Tuff and together comprise the nonwelded Paintbrush Tuff (PTn) (Fig. 1). The Pah Canyon Tuff varies from welded to moderately welded and has a maximum thickness of 78 m in the north part of Yucca Mountain (Stuckless and Dudley, in press). The Yucca Mountain Tuff is non-welded throughout much of the Yucca Mountain area and reaches 45 m in thickness. The PTn is an important hydrogeological unit as flow changes from fracture flow in the overlying Tiva Canyon Tuff, to matrix flow in the PTn (Stuckless and Dudley, in press). The Pah Canyon and Yucca Mountain Tuffs are overlain by the Tiva Canyon Tuff, dated at 12.7 Ma (Sawyer et al. 1994) and composed of lower crystal-poor and upper crystal-rich members. The Tiva Canyon Tuff reaches a thickness of 175 m. After deposition of the Paintbrush Group, Basin and Range extension generated normal faults that cut the sequence (e.g. Stewart, 1988) (Fig. 1). Basaltic volcanism generated cinder cones during the late Tertiary and formed the recent Lathrop Wells Cone at around 77 Ka (Heizler et al., 1999). Detailed descriptions of the geology at Yucca Mountain are given by Sawyer et al. (1994), Buesch et al. (1996), and Stuckless and Dudley (in press).

The Exploratory Studies Facility (ESF) was excavated through the Tiva Canyon Tuff, PTn, and Topopah Spring Tuff to allow characterization of the volcanic stratigraphy (Figs. 1 and 2). To further examine the Topopah Spring Tuff, which is the potential repository horizon, and the Solitario Canyon fault zone a second tunnel, the Enhanced Characterization of the Repository Block Cross Drift (ECRB), was constructed (Mongano et al., 1999). The ECRB was excavated entirely within the Topopah Spring Tuff and trends northeast to southwest about 15 m above the potential repository site.

The potential repository horizon is about 300 m below the surface and approximately 200 – 400 m above the water table. At Yucca Mountain the UZ extends from the surface to depths of 500 – 700 m where the water table is encountered and the saturated zone (SZ) begins (Fig. 1). The barren zone (BZ) straddles the UZ and SZ and contains minor calcite relative to other regions. The top of the barren zone is approximately 100 - 300 m above the water table and it extends to approximately 400 m below the water table (Vaniman and Chipera, 1996). Underlying the BZ and at depths greater than 1 km is the calcite alteration zone (CAZ), characterized by tuffs and lavas that are altered to carbonate-bearing assemblages that have chemically distinct Mn-rich calcite (Denniston et al., 1997). The shallower part of this zone contains analcime and calcite, whereas albite and calcite dominate at greater depths (Bish and Chipera, 1989). The upper boundary of the CAZ appears to be the upper boundary of an 11 Ma fossil hydrothermal zone beneath Yucca Mountain (Bish, 1989). The majority of CAZ calcite forms pseudomorphs after feldspar phenocrysts within the rock matrix (Caporusico et al., 1982) and the calcite-albite-quartz-barite alteration assemblage indicates formation at about 250 °C (Vaniman, 1994).

Secondary minerals within the UZ are restricted to the footwalls and bases of LC, fractures, and breccias (Whelan et al., 1996). LC are roughly bedding parallel and formed as gases exsolved during deposition and cooling of the tuffs. Exsolving high temperature fluids altered the margins of LC and cooling fractures, producing distinctive bleached halos and vapor-phase veinlets consisting of tridymite, cristobalite, alkali feldspar, hematite and other accessory minerals subparallel to bedding (Carlos, 1994; Levy et al., 1996). Lithophysal cavities are

commonly connected by fine fractures, some of which are altered by vapor-phase mineralization. Fracture types include early cooling joints and later tectonic joints which have similar near vertical orientations, and joints that formed in response to erosional unloading (Stuckless and Dudley, in press). Breccias have variable features, some of which are associated with fault zones across the site.

3. PREVIOUS RESEARCH

3.1. Petrographic and Paragenetic studies

Previous petrographic studies documented the presence of a variety of calcite morphologies (Whelan et al., 1994; Dublyansky, 1998; Whelan and Moscati, 1998). A generalized paragenetic sequence presented by Whelan et al. (in press), which evolved over several years (e.g. Whelan et al. 1994; 1998; 2000; Paces et al., 2001), indicates initial high-temperature deposition of vapor-phase tridymite and hematite along cooling joints, fractures, and at the bases of LC. Early deposition of calcite, fluorite, and chalcedony-quartz was followed by intermediate and late deposition of calcite with minor opal. Whelan et al. (in press) documented the presence of distinctive bladed calcite with scepter overgrowths of clear 'late stage' calcite. The authors suggested that this general paragenetic sequence could be correlated across the site based on similar trends in $\delta^{13}C$ and $\delta^{18}O$ values (Whelan et al., 1998), comparable $^{230}Th/U$ and U-Pb ages of opal from fracture and LC occurrences (Paces et al., 2001), and the similarity in parageneses of secondary minerals in shallowly dipping fractures and adjacent LC (Paces et al., 2001).

Dublyansky et al. (2001) discussed secondary minerals but did not provide detailed petrographic descriptions or paragenetic relationships. Limited petrographic observations are, however, consistent with the paragenesis presented by Whelan et al. (in press).

3.2. Cathodoluminescence

Previous cathodoluminescence studies of Yucca Mountain calcite are limited; Denniston et al. (1997) studied calcite from the UZ and CAZ and Whelan et al. (1994; 2000; 2001) studied UZ calcite. Denniston et al. (1997) observed 1 – 20 μm alternating luminescing and nonluminescing bands in UZ calcite. Suture-form discontinuities between domains of fine bands indicated a hiatus between events of calcite precipitation. Whelan et al. (1994) examined drill core samples and observed that some UZ calcite displayed orange luminescent growth zoning. Preliminary observations by Whelan et al. (in press) indicated that some of the early-stage calcite and most of the late-stage calcite display fine growth zoning defined by orange luminescence and white UV fluorescence. They further observed that intermediate-stage calcite contained only widely separated luminescent growth zones in a non-luminescent background.

3.3. Calcite Composition

The chemical composition of calcite in the UZ and SZ was investigated in drill core samples by Vaniman (1993; 1994) using electron microprobe and instrumental neutron activation analyses. Prominent negative Ce and Eu anomalies and low concentrations of transition metals (Fe, Mn, Mg, and Sc) were observed only in UZ calcite. These variations distinguished UZ calcite from

SZ calcite. Investigation of trace elements in the calcite from drill core samples by electron microprobe, ICP-MS, and secondary ion mass spectrometry (Denniston et al., 1997) showed that UZ calcite had small variations in REEs and that Mn, Fe, and Sr abundances varied considerably within most calcite samples. Samples from the UZ were depleted in Mn, were similar to samples from the soil zone, and were clearly different from Mn-enriched CAZ samples (Denniston et al., 1997). Denniston et al. (1997) observed that CAZ calcites contained flat Ce patterns and minimum negative Eu allowing them to be differentiated from UZ calcites.

3.4. Stable Isotopes

Previous C and O isotopic studies of micro-sampled calcite from secondary minerals crusts (Whelan and Moscoti, 1998; Whelan et al., in press) showed that $\delta^{13}C$ decreased from about 10 ‰ in early calcite to -8 ‰ in late-stage calcite, as $\delta^{18}O$ increased from about 13 ‰ in early calcite to 20 ‰ in late-stage calcite. In spite of this general trend, the ranges of values determined for early, intermediate, and late calcite are not unique, and isotopic signatures cannot be used to determine the age of the calcite (Whelan et al., in press). Nevertheless, their data suggest general trends: calcite older than 4 Ma has $\delta^{13}C$ values greater than -4 ‰ and calcite younger than 1 Ma has $\delta^{13}C$ values less than -4.5 ‰ (Paces et al., 1997; Whelan et al., in press). Early calcite that had $\delta^{18}O$ compositions of less than 10 ‰ was interpreted to have formed from fluids with temperatures of 50 – 80 °C (Paces et al., 1997; Whelan et al., in press). $\delta^{18}O$ signatures of later calcite were interpreted to be compatible with deposition of secondary minerals from local meteoric or ground waters (Paces et al., 1997). $\delta^{13}C$ compositions were interpreted to indicate surficial sources for carbon dissolved in the downward-percolating solutions (Paces et al., 1997). This interpretation is supported by the similarity between the C and O isotopic signatures obtained from overlying pedogenic carbonates and the calcite from secondary mineral crusts (Whelan et al., in press).

Dublyansky et al. (2001) presented limited C and O isotope data for mineral crusts from vertical fractures in the Tiva Canyon Tuff from near the north portal of the ESF. $\delta^{18}O$ varied between 18.5 – 20.0 ‰ (conversion to $\delta^{18}O_{VSMOW}$ after Coplen et al., 1983) and in most samples compositions were consistent across the calcite crusts. $\delta^{13}C$ compositions for calcite were typically negative (Dublyansky et al., 2001). These ranges in $\delta^{18}O$ and $\delta^{13}C$ are narrower than ranges obtained by the USGS, and contrast with isotopic data from samples across the site (Whelan et al., in press). A comparison of the two data sets suggests that results by Dublyansky et al. (2001) from a limited part of the ESF probably only reflect part of the paragenetic sequence of the mineral crusts.

4. METHODOLOGY

4.1. Sample Collection

One hundred and fifty-five samples of secondary minerals and adjacent wall rock were collected from LC, fracture, and breccia occurrences from the ESF, ECRB, and exploration alcoves at Yucca Mountain. Sample locations are shown in Figure 2. The sample suite is representative of secondary mineral occurrences at Yucca Mountain. Samples collected in the tunnels were wrapped in aluminum foil, placed in cloth bags, and transported in a cooler to minimize

temperature variations. Because previous fluid inclusion studies indicated that homogenization temperatures could be as low as 35 °C, samples were kept between 0 – 35 °C in accordance with quality assurance (QA) procedures. Within this restricted temperature range fluid inclusions in the samples are unlikely to be modified owing to freezing or overheating.

4.2. Thin Section Preparation and Petrography

Owing to their fragile nature, samples selected for polished sections were impregnated with room temperature curing epoxy under vacuum. Samples were cut using a Buehler Isomet® slow speed saw with a Buehler® diamond wafering blade. Doubly polished thick sections (DPTS) were ground to a thickness of approximately 200 μm using a Hilquist® diamond cup wheel. Water was used for all cutting, grinding, and polishing steps to keep the sections cool. Final polishing by hand produced sections approximately 100 μm thick. A total of 5 sections were made from each billet. Two sections were used in this study; one of the sections was used for microprobe investigations and the other section was used for all other analyses. Of the remaining three sections, one was prepared for the State of Nevada and two were prepared for the USGS to provide equivalent sample material, produced under sample QA procedures, for independent studies.

Images of the sections were created using an Olympus slide scanner and/or Visioneer 7600 flatbed scanner to record the sections and assist with the petrographic studies. Petrographic investigations were made using Olympus BX-60 and Nikon OPTIPHOT-POL microscopes. Photomicrographs were captured using a Polaroid DMC IE digital camera.

4.3. Electron Microprobe

Quantitative analyses and qualitative X-ray maps were produced using a JEOL JXA-8900R Electron Probe Microanalyzer at UNLV. Natural standards (dolomite, calcite, strontianite, siderite, and rhodonite) were used for calibration and as reference materials. Quantitative point analyses were performed using an accelerating voltage of 10 kV, 7 nA probe current, and a 10 μm beam diameter with a 10 second counting time. Qualitative X-ray maps were collected with a single pass, dwell time of 20 ms, accelerating voltage of 15 kV, and a 20 nA probe current.

4.4. Cathodoluminescence

Cathodoluminescence studies were conducted using an automated 8200 Mk4 Cambridge Image Technologies Limited (CITL) cold cathodoluminescence stage, with an accelerating potential of 15 – 20 kV, beam current of 400 – 600 μA, and chamber vacuum of about 20 mbar. The stage was attached to a Nikon OPTIPHOT-POL microscope with a Nikon FX35-DX camera and an automatic AFX-DX controller. Photomicrographs were obtained using 1600 ASA/ISO color film.

4.5. LA-ICP-MS

Laser ablation inductively coupled plasma mass spectrometry (LA-ICP-MS) was performed on a Micromass® Platform ICP-HEX-MS quadrupole mass spectrometer with ICP ion source and hexapole collision cell, for removal of interfering polyatomic ion species, integrated with an in-

situ Merchantek® UV laser ablation microprobe. National Institute of Standards and Technology (NIST) glass standard reference materials were used as standards and in calibration of the ICP-MS (sample reference materials 610 (500 ppm), 612 (50 ppm), 614 (1 ppm), and 616 (0.02 ppm). Signals were collected for the instrument blank without firing the laser, and then collected on material ablated from 3 NIST glass standards for 200 milliseconds. Signal collection was repeated for 1 minute for each standard and all signals were integrated. Unknown samples were analyzed and concentrations were calculated from equations of lines generated by blanks and standards and corrected for matrix and drift correction and interfering polyatomic ion species.

4.6. C and O isotopes

Samples for C and O isotope analyses were drilled from DPTS using a Merchantek Micromill. Milled samples were typically 100 – 150 μg and were collected with a scalpel blade and placed in labeled polyethelene microcentrifuge tubes. Drill paths were digitized onto digital images of the samples.

Powdered calcite samples were roasted under vacuum for one hour at 380 °C to remove volatile components and stored in a desiccator. Desiccated sample powders were loaded into individual borosilicate or quartz reaction vessels used in an automated Finnigan® Kiel III Carbonate Device. Samples were reacted with 2 drops of anhydrous H_3PO_4 at 74 °C. Resultant water and CO_2 were cryogenically separated and pure CO_2 was transferred to a micro-volume for introduction to a Finnigan® MAT 252 isotope ratio mass spectrometer for analysis. Isotopic measurements were performed at the University of Iowa and were calibrated against laboratory reference gas (LASIS). All carbonate CO_2 isotopic analyses were corrected for ^{17}O contribution and acid fractionation effects. Results are expressed as ‰ deviation; $\delta^{13}C$ values were reported relative to V-PBD, and $\delta^{18}O$ values are reported relative to VSMOW. Analytical precision is greater than ± 0.1 ‰ for both carbon and oxygen isotope ratios and was monitored through daily analysis of duplicate sample aliquots and powdered carbonate standards (NBS-18, 19, 20 and other in-house carbonate standards).

5. MINERALOGY AND PETROLOGY

5.1. Mineral Occurrences and Spatial Variations

An important observation at Yucca Mountain is that most fractures, breccias, and LC do not contain secondary minerals. In sites where secondary minerals are present, these minerals fill only a fraction of the available open space and form thin (2 - 3 mm) crusts. At outcrop scale, mineral phases and abundances vary significantly at each sample site and across the site.

During sampling it was noted that the secondary mineral habits and abundances correlate, to some degree, with host lithology and sample location. Secondary minerals in the Tiva Canyon Tuff and upper nonlithophysal unit of the Topopah Spring Tuff in the north portal and ramp (NPR; Fig. 2) are generally present in fractures and breccias. Where present, the secondary minerals usually fill the available open space and are dominated by chalcedony, quartz, and opal rather than calcite. Some samples also contain significant fluorite. Lithophysal cavities are the predominant site for secondary minerals in the lithophysal cavity zone (LCZ; Fig. 2) which occurs in the upper lithophysal unit and lower nonlithophysal unit of the Topopah Spring Tuff.

This locality exhibits some of the thickest crusts, which are dominantly calcite with lesser opal, chalcedony, and quartz. Samples collected in the intensely fractured zone (IFZ; Fig. 2) are from the lower nonlithophysal unit of the Topopah Spring Tuff and contain only calcite with minor fluorite along thin fractures. In the south portal and ramp (SPR; Fig. 2) samples were collected from units between the lower nonlithophysal unit of the Topopah Spring Tuff and the Tiva Canyon Tuff. These samples are from fracture, LC, and breccia occurrences and contain calcite, chalcedony, quartz, minor opal and fluorite. ECRB cross drift (ECRB; Fig. 2) samples were collected from LC in the upper lithophysal to lower nonlithophysal units of the Topopah Spring Tuff, and consist primarily of calcite with minor opal, chalcedony, and quartz. A few fracture and breccia samples contain calcite. Samples collected from alcoves 6 and 7 are dominantly fracture and breccia samples, probably owing to proximity to the Ghost Dance Fault. These samples primarily contain calcite.

In thin section differences between samples from LC, breccias and fractures are apparent (Fig. 3). Crusts from LC can reach 4.5 cm in thickness and exhibit some of the most complex mineral stratigraphies observed (Fig. 3a). In many cases, however, LC samples are comprised of a single calcite habit (Fig. 3b; bladed calcite), or exhibit thin layers of calcite (Fig. 3c) that average 0.5 cm in thickness. In general, thicker crusts exhibit multiple layers (e.g. Fig. 3a; 3 layers) with distinctly different textures that are related to different generations of mineral precipitation. Fractures can contain thin calcite crusts (Fig. 3d) or thicker complex crusts (e.g. Figs. 3e and f). Steeply dipping fractures from the Topopah Spring Tuff commonly contain thin layers of calcite. Fractures from the NPR and SPR contain complex crusts and with significantly more silica mineralization than other sample locations. The silica phases typically occur adjacent to the wall rock and were overgrown by later calcite (Fig. 3e). Breccia samples (Figs. 3g to i) may contain abundant open space. In Figure 3g, two mineral crusts exhibit finer grained, thin layers of calcite at the base, that were overgrown, in turn, by coarser, slender bladed calcite and clear sparry calcite. Such samples are paragenetically equivalent to many LC samples. Other breccia samples are composed of fine to coarse pieces of tuff cemented by calcite. In most cases these breccias are only partially cemented by thin rims of calcite that line pore spaces, suggestive of meniscus textures, and abundant open space is present between adjacent tuff pieces (Figs. 3h and i). Smaller pores were typically filled, whereas larger pores are only partially filled. As Figure 3 illustrates, abundant porosity is associated with all occurrences of secondary minerals at both micro and macro scales.

5.2. Petrography

During the paragenetic study, the occurrences and habits of the older and intermediate calcite were observed to be variable. For example, some samples are composed of primarily bladed calcite that precipitated directly on the wall rock (e.g. sample ESF 28+81; Fig. 3b), whereas in other samples primarily blocky calcite is present (e.g. sample ECRB 10+10). In contrast to the variability of older phases, younger secondary minerals were observed to be relatively continuous across the repository site. In particular, a chemically distinct sparry calcite, that contains fine Mg-enriched growth zones (termed Mg-enriched growth-zoned sparry calcite (MGSC); see section 6.1) forms the outermost mineral layer in most of the samples. The continuous nature of this MGSC indicates that the younger history of calcite deposition at Yucca Mountain was consistently recorded across the site.

A comparison of all samples, patterns of mineral deposition, and textural relationships shows that the various calcite habits reflect the timing of mineral deposition. This comparison further demonstrated that no single location or sample recorded the entire history of secondary mineralization, indicating that processes responsible for secondary mineral deposition did not occur uniformly throughout the repository horizon. As a result, a relatively large number of samples must be examined in order to identify all depositional events and periods of non-deposition, and to determine the relative timing of deposition of the various mineral events.

5.2.1. Calcite

Calcite is the most abundant mineral within LC, fractures and breccias, occurs throughout the mineral paragenesis, and makes up more than 95% of all secondary minerals within the site.

Basal calcite in LC, which is somewhat variable, is commonly overgrown by bladed calcite, and subsequently by MGSC, the outermost layer of calcite in most mineral crusts. Basal calcite forms irregular, interlocking, subhedral crystals adjacent to the wall rock (Fig. 4a). This early calcite commonly overgrows tuff fragments and is typically finer-grained and darker than most younger calcite. Basal calcite also occurs as blocky calcite containing numerous tuff fragments and fluid inclusions. This calcite exhibits cleavage (Fig. 4b) and, at some localities, has no distinctive characteristics.

Bladed calcite occurs as small bladed and longer bladed crystals that comprise the majority of LC crusts. The abundance of bladed calcite may be, in part, a function of available open space. These crystals are also present in fracture and breccia samples, overgrowing earlier basal calcite in all occurrences.

A single, chemically distinctive calcite layer, MGSC (see section 6.1) consistently forms the outermost and youngest mineral layer across the site. MGSC forms both clear calcite and dark patchy calcite (Figs. 4c and d) delineating growth zones. The dark growth zones can contain rare, liquid-only fluid inclusions and are locally highlighted by intergrowths of opal (Fig. 4e). The dark color observed in some samples probably results from microporosity along the growth zones. In samples in which MGSC is not present, textural relationships indicate that MGSC did not precipitate, and the sample site did not record the complete history of secondary mineral precipitation. For example, bladed calcite overgrown by MGSC is evident in Figures 4c and 4f; in Figure 3b, however, bladed calcite forms the outermost mineral layer. MGSC is not present and, therefore, did not precipitate at this site.

In fracture and breccia occurrences, the earliest calcite adjacent to the wall rock is usually finely layered calcite (Fig. 4g) which contains tuff fragments and, at some localities, small cubic fluorite inclusions. In some samples from the IFZ, fluorite was the first secondary mineral to precipitate on the wall rock and was overgrown by multiple later generations of calcite (Fig. 4h). Layered calcite is present in fractures and breccias in the Topopah Spring Tuff, but has not been observed in samples from the Tiva Canyon Tuff. Layered calcite is overgrown by calcite exhibiting a number of different habits including fine dark, bladed calcite, clear calcite, and MGSC. As observed in LC, the outermost calcite in many fracture occurrences is MGSC (Figs. 4d and i).

All of these observations indicate a similar paragenesis for LC and fracture and breccia occurrences, although certain mineral layers tend to be thicker or thinner, or present or absent at various sample localities. Paragenetic relationships are particularly consistent in the ECRB

where samples from LC, fractures, and breccias have identical parageneses and all samples exhibit bladed calcite overgrown by MGSC.

5.2.2. Opal

Opal is colorless to dark brown (nearly opaque) in plane polarized light (Figs. 4c - e) and occurs as thin layers and isolated hemispheres. Under short-wave UV light and CL, outer clear opal and some brown opal fluoresce and luminesce bright green, respectively, highlighting the growth layering in the samples.

Brown opal commonly occurs in the older basal portions of secondary mineral crusts (Figs. 4d, i and j) and clear opal occurs in the younger central and outer parts of the crusts (Figs. 4c and e), however, young brown opal and old clear opal have been observed (Wilson et al., 2002). Brown opal is typically associated with early chalcedony and quartz and rarely with fluorite, and forms distinct layers and irregular masses. This opal is common in fractures in the NPR and SPR where it is usually associated with chalcedony (Fig. 4d). The presence of inclusions of anhedral calcite in opal at the base of mineral crusts, and irregular boundaries between opal and calcite suggest some dissolution of calcite and replacement by opal. In most fracture occurrences brown opal is overgrown by MGSC (Fig. 4d).

Most clear opal is intergrown with MGSC in the outer part of the crusts. This opal occurs as both continuous and discontinuous layers and as isolated hemispheres and clusters of hemispheres (Figs. 4c and e). Within MGSC, multiple distinct opal layers can be present (Figs. 4c and e). Calcite is optically continuous across these opal layers which can vary in thickness. The contact between opal and underlying calcite is usually planar but in some samples, dissolution of the underlying calcite and replacement by opal is indicated. The presence of opal layers and hemispheres aligning growth zones in the calcite, and the presence of adjacent opal and calcite that exhibit serrated contacts in the growth direction (Fig. 4e) suggest that, at some localities, opal and calcite are coeval. However, in other samples opal layers cut across growth zones in MGSC (Fig. 4c).

5.2.3. Chalcedony

Chalcedony occurs as layered or massive radial growths of crystallites (Figs. 4f, i, and j). Chalcedony commonly exhibits bright green fluorescence under short wave UV light, but the fluorescence is often masked by the stronger fluorescence of associated brown opal.

Chalcedony is commonly spatially associated with quartz and, at most localities, euhedral quartz crystals precipitated on outermost chalcedony (Fig. 4j). In fact, chalcedony commonly appears to form 'roots' at the base of euhedral quartz crystals. A number of observations indicate that chalcedony replaced earlier calcite. These include irregular boundaries between chalcedony and underlying calcite (Figs. 4f and i; Fig. 5b), the presence of inclusions of anhedral calcite in chalcedony (white arrows in Fig. 4i), and pseudomorphs of calcite cleavage in the chalcedony (black arrows in Fig. 4i).

In LC samples, chalcedony forms layers associated with brown opal (Fig. 4j). Chalcedony commonly occurs as thick layers in the NPR and SPR (Figs. 4d and i), and is most common in the NPR. In fractures, chalcedony is intergrown with opal, and multiple generations of chalcedony and opal are commonly present (Fig. 4j). Chalcedony is not associated with MGSC in the outermost part of mineral crusts. This relationship is significant in that it constrains

chalcedony to be paragenetically early to intermediate in age, consistent with dates obtained using U-Pb methods (Wilson et al., 2002).

5.2.4. Quartz

Quartz occurs primarily as small, euhedral crystals adjacent to the wall rock and associated with chalcedony and brown opal in the basal parts of crusts in all sample occurrences (Figs. 4i – k). 'Roots' of chalcedony commonly form the base of euhedral quartz crystals, but clusters of quartz crystals can occur without associated chalcedony. At some localities, particularly in the NPR, quartz adjacent to the wall rock contains inclusions of fluorite (Fig. 4k). At some sample locations quartz has not been overgrown by later minerals, and drusy quartz forms the outermost mineral layer. However, in most samples quartz is overgrown by later minerals and ultimately by MGSC, indicating quartz is early to intermediate in age.

5.2.5. Fluorite

Fluorite occurs as cubic and irregularly shaped inclusions (Fig. 4k), nodular growths (Fig. 4k), continuous and discontinuous layers (Fig. 4h), hemispherical masses, and as massive cements around tuff pieces within fractures, breccias, and LC. Under plane polarized light fluorite is usually clear, but fluorite can be purple and exhibit growth zoning. Fluorite typically exhibits massive and nodular forms that precipitated around vapor-phase minerals, wall rocks, and at the base of the secondary crusts. In LC samples, small cubic inclusions of fluorite occur within calcite at the base of the crusts adjacent to the wall rocks. Fluorite has not been observed in MGSC. The presence of fluorite both at the base of secondary minerals and within early calcite, and the lack of fluorite in MGSC suggests that more than one episode of fluorite precipitation occurred, but that all episodes were early to early – intermediate in age.

6. CHEMICAL COMPOSITION

6.1. Microprobe Analyses

Electron microprobe studies included quantitative wavelength dispersive spectrometry (WDS) point analyses using extended count times over the entire spectra of elements, and using shorter count times over a specific range of elements (Sr, Mn, Fe, Mg, K, Ca, Al, U, Si, and F). Early results showed that the majority of the calcite (80 – 90 %) does not contain significant and consistently detectable trace or minor elements using EPMA. However, Mg was detected in the majority of samples in early calcite and late MGSC. Quantitative analyses determined that Sr, Fe, and Mn were present at low levels. Typically calcite (e.g. basal, bladed, and MGSC) contained concentrations of these elements at levels below detection limits to around 0.4 – 0.7 wt. % for Sr, 0.3 – 0.7 wt. % for Mn, and 0.4 – 0.9 wt. % for Fe. The presence or absence of these elements does not coincide with calcite habit and concentrations are comparable in all calcite types. Strontium and Mg show fairly even distributions, whereas Mn and Fe are more variable. X-ray mapping did not show any consistent growth-related variation in Sr, Mn, or Fe; however, in a few samples, Mg and Sr were negatively correlated. In contrast, Mg is clearly related to specific calcite habit and paragenetic stage. Quantitative analyses of opal, chalcedony,

quartz, and fluorite did not show any consistent variations in trace or minor elemental compositions.

Electron microprobe X-ray mapping of the majority of samples revealed the presence of chemically distinct Mg-enriched calcite that could be correlated across the site. Magnesium-enriched calcite exhibits two morphologies: irregular Mg-enriched patches in early calcite and complex oscillatory growth zoning in late sparry calcite (Fig. 5). Mg-enrichment in calcite that does not display growth zoning is termed patchy Mg-enriched calcite (PMC). PMC usually occurs adjacent to vapor-phase minerals, commonly tridymite, fluorite, and around the wall rock at the base of the secondary crusts (Figs. 5a and b). In some samples PMC occurs in outermost calcite, but this is because in these samples only older calcite is present, which has not been overgrown by younger secondary minerals. Patchy Mg-enrichment varies in thickness over short distances and is discontinuous. Unlike Mg-enriched growth zoning, PMC cannot be clearly related to crystal habit; however, PMC is not observed in bladed or outer sparry calcite and it is restricted to paragenetically early calcite. PMC contains up to 1.3 wt. % MgO, however, concentrations vary across patches (Figs. 5a and b).

Calcite that contains Mg-enrichment that displays growth zoning is referred to as magnesium-enriched growth-zoned sparry calcite, or MGSC. More than 120 samples were X-ray mapped, typically for Mg, Fe, Sr, and Mn, and the outermost layer in more than 65 % of these samples is MGSC. Mg-enriched growth zoning always occurs in outer sparry calcite and more than 75 % of the collected samples contain MGSC. These samples include 65 % of the samples that were X-ray mapped and an additional 10 % of the samples that contain readily identifiable MGSC (i.e. visible growth zones, sparry habit, and associated clear opal).

MGSC (Figs. 5b and c; Fig. 6) contains numerous oscillatory growth zones that are typically ~50 to 100 μm thick, but which thicken locally. Individual MGSC growth zones are planar and asymmetrically around crystal axes, and overgrow earlier minerals that do not contain Mg (Figs. 5b and c; Fig. 6). Within MGSC the Mg composition varies from below the detection limit to around 1 wt. % Mg; however, this range can vary along individual growth zones.

The thickness of the MGSC layer ranges from hundreds of micrometers to centimeters at various sample sites. Where present in the NPR and SPR, MGSC commonly occurs as thin to thick (≥ 0.5 cm) layers. In the LCZ and ECRB, MGSC is present in the majority of samples. The layer is commonly less than 0.5 cm at these localities; however, the thickness of the MGSC overgrowths can vary considerably between adjacent sample localities. MGSC occurs as thin overgrowths (typically less than 500 μm) in the southern part of the IFZ, but MGSC is rare in other parts of the IFZ.

The consistent presence of this mineral layer and its occurrence as the youngest secondary mineral reflects a single site-wide precipitation event. The variability in the detailed growth zoning and thickness of this layer in different samples limits development of a 'cement stratigraphy' that can be correlated from sample site to sample site. Nevertheless, MGSC forms a single micro-stratigraphic unit that reflects a geologically recent fluid flow event across the site.

6.2. Cathodoluminescence

Cathodoluminescence is observed in the calcite crusts, but has not been as diagnostic as chemistry in correlating secondary minerals across the site because it is more variable. Cathodoluminescence investigations focused on calcite, opal, and fluorite because quartz, chalcedony and vapor-phase minerals did not luminesce.

Most calcite is not luminescent. Calcite that does luminescence exhibits fine (~ 50 μm), planar to curved, irregular, and oscillatory (Fig. 4l) orange growth zones within some crystals, with more massive luminescence zones, where fine growth zones are not observed, along grain boundaries and within some crystals. Similar colors and intensities are generally observed. Luminescence highlights discontinuous growth zoning revealing precipitation breaks in optically continuous calcite.

All samples from the IFZ exhibit the most strongly luminescent and complex growth zoning (Fig. 4l). Luminescence in layered calcite adjacent to the wall rock is common in these samples and this calcite is typically overgrown by calcite exhibiting oscillatory luminescent growth zoning. Thin, concentric luminescent growth zones highlight partially filled pore spaces and indicate a pore filling texture.

Generally, early calcite that rims vapor-phase minerals in LC is luminescent. Bladed calcite can contain luminescent growth zoning and is luminescent along grain boundaries. Typically MGSC is not luminescent, but in some samples fine luminescent growth zoning is present. This luminescence coincides with growth zones visible under transmitted light and those observed in MGSC, but does not occur in many samples. Typically, samples from the ECRB exhibit more luminescence throughout the crust than similar samples from the ESF.

Outer clear opal generally exhibits bright green luminescent growth zoning with some layers luminescing much more strongly than the majority of the opal. Fluorite exhibits green luminescent growth zones and, locally, this luminescence reveals discontinuities related to fluorite dissolution and re-precipitation.

6.3. LA-ICP-MS Analyses

LA-ICP-MS analyses of MGSC, luminescent, non-luminescent, and basal calcite did not identify any significant elemental variations at levels below detection levels of the EPMA. Analyses showed that there is some enrichment in MGSC of U, Th, and Sr compared to calcite from the inner parts of the samples. However, this variation was not consistent. Orange luminescence commonly reflects the presence of Mn^{2+} as an activator (Machel et al., 1991), but variations in Mn^{2+} were not confirmed using LA-ICP-MS analyses and both non-luminescent and luminescent calcite contained similar amounts of Mn.

6.4. C and O Isotope Analyses

Eighty micro-samples of calcite from different stages were collected from across the repository site, and were analyzed for C and O isotopic compositions. The results are given in Table 1 and shown in Figure 7. Samples exhibit ranges for $\delta^{13}C$ from -8.5 to 9.5 ‰, and for $\delta^{18}O$ from 5.2 to 22.1 ‰. Samples exhibit generally consistent trends in C and O isotopes from paragenetically early calcite to the younger and outermost parts of the crusts. Most older calcite has lower $\delta^{18}O$ compositions, which increase in the younger minerals (Table 1; Fig. 7). Alternatively, $\delta^{13}C$ compositions decrease from positive values in older calcite at the base of crusts to negative values around -6.0 to -8.0 ‰ in the youngest calcite. All $\delta^{18}O$ and $\delta^{13}C$ data have a negative correlation of $r = -0.72$.

MGSC has relatively consistent signatures of 16 – 20 ‰ for $\delta^{18}O$ and -3.0 to -8.5 ‰ for $\delta^{13}C$. However, these signatures are not diagnostic because samples of bladed, intermediate, and outermost non-descript calcite can have similar isotopic compositions (Fig. 7). Bladed calcite

exhibits a very large range in $\delta^{13}C$ of about 18 ‰ and the higher end of this range overlaps with signatures determined for MGSC. Intermediate calcite from the central parts of crusts also has a wide range of carbon isotope compositions, generally similar to bladed calcite and this range of signatures also overlaps with isotopic signatures determined for MGSC. Outermost calcite that is not Mg-enriched, and which has no distinguishing characteristics, has similar isotopic compositions to MGSC, but exhibits a somewhat shifted range in $\delta^{13}C$. The net result is that several morphologically distinct types of intermediate and outer calcite have similar isotopic compositions, even though paragenetic relationships show conclusively that the absolute ages of these calcites are different.

Filled symbols on Figure 7 identify isotopic signatures of calcite samples that are spatially associated with two-phase fluid inclusions (Wilson et al., 2002) and the symbols correspond to the habit and/or relative paragenetic position of the calcite. Most two-phase fluid inclusions occur in basal, bladed and intermediate calcites that have positive $\delta^{13}C$ compositions (Fig. 7). A few basal and intermediate calcites associated with two-phase fluid inclusions have $\delta^{13}C$ compositions as low as -3 ‰. These samples also have low $\delta^{18}O$ compositions that are less than values determined for MGSC. It is significant that samples of bladed calcite that contain two-phase inclusions have carbon isotopic signatures that are distinctly different from bladed calcite that contains only 1-phase inclusions (Fig. 7; Wilson et al., 2002). This is suggestive that bladed calcite precipitated over a prolonged period of time from a fluid that varied in temperature and isotopic composition.

7. PARAGENESIS

By integrating the petrographic observations with EPMA, cathodoluminescence, LA-ICP-MS, and C and O isotopes it is possible to better constrain the paragenetic sequence for secondary minerals in each sample, and to link these parageneses across the site. Although there is significant mineralogical variability, particularly in the older parts of the crusts, a paragenetic framework that displays consistent textural relationships for secondary minerals in all samples can be constructed. Vertical slices through Figure 8 at various points across the diagram represent individual parageneses observed at various sample sites. Collectively, these parageneses illustrate the history of secondary mineral precipitation across the site, highlight significant mineral relationships, and illustrate the variation between individual sample sites with respect to early stages of secondary minerals and the consistency of latest MGSC.

7.1. Paragenesis of Lithophysal Cavities

After the tuff was deposited, vapor-phase minerals (tridymite, drusy quartz, platy hematite, ± fluorite?) formed adjacent to the wall rock and were overgrown by early fluorite. Fluorite occurs as nodular growths around the wall rock and can also form massive cement around tuff pieces. Tuff, vapor-phase minerals, and fluorite were overgrown by calcite that exhibits a variety of habits. For example, some samples contain basal blocky calcite with distinctive cleavage (Fig. 8c) and which cements tuff pieces, overgrown by small bladed calcite (Fig. 8c), irregular calcite grains (Fig. 8b), clear calcite, and dark inclusion-rich (i.e. tuff, mineral and lesser fluid inclusions) calcite (Fig. 8c). Basal calcite is usually finer-grained than calcite in outer parts of the crusts (Figs. 8b and c). These early calcites locally contain cubic fluorite crystals or, rarely, clear

opal hemispheres (Fig. 8b). Some basal calcite contains patchy Mg-enrichment around fluorite and tridymite, but outboard of this basal calcite, significant trace elements, other than in MGSC, are not detected (see Fig. 5b). Basal calcite is commonly luminescent and exhibits oscillatory growth zones at the base of crusts and along some grain boundaries. C and O isotopic signatures for basal calcite typically have positive $\delta^{13}C$ and $\delta^{18}O$ below about 17 ‰ (Fig. 7).

Some LC samples, primarily those from the ESF, contain a quartz-chalcedony-brown opal layer. This layer may consist of fine chalcedony overgrown by euhedral quartz crystals (Fig. 8d) or, alternatively, a relatively thick layer of intergrown chalcedony and brown opal overgrown by quartz crystals (Fig. 8e). Dissolution and replacement of earlier calcite by quartz-chalcedony-brown opal (Fig. 8e) are indicated by highly irregular boundaries between the silica minerals and the underlying calcite, and the presence of isolated, but optically continuous anhedral calcite inclusions in the chalcedony-quartz (Fig. 8e). In some samples chalcedony-quartz-brown opal contains fluorite. Chalcedony-quartz-brown opal generally occurs in a single layer in LC, whereas multiple layers are common in fracture occurrences (see Fig. 4d). The silica layer overgrows earlier calcite as well as earlier vapor-phase minerals. Virtually all two-phase fluid inclusions observed during this study were present in basal calcite below, and paragenetically older than, the silica layer (Wilson et al., 2002).

Bladed calcite precipitated on early calcite or silica and is present in virtually all LC samples in the ESF and ECRB (Fig. 8f). Where bladed calcite occurs, silica is typically minor and bladed calcite comprises the majority of these crusts (Fig. 8o). Where calcite blades form overgrowths on earlier calcite, the overgrowths are usually optically continuous. Early, inner cores of bladed calcite crystals rarely contain two-phase fluid inclusions, whereas the middle and outer parts of the blades contain only rare, liquid-only inclusions (Wilson et al., 2002) and have different C and O isotopic compositions (Fig. 7). Petrography and C and O isotopic trends indicate that bladed calcite that contains two-phase fluid inclusions is older than bladed calcite that contains liquid-only inclusions. Virtually all bladed calcite is free of consistent trace element variations detectable by EPMA; however, this calcite does locally luminesce along growth zones and crystal boundaries.

Where present, MGSC and locally intergrown opal overgrow and exhibit consistent relative age relationships with all other secondary minerals (Figs. 8g – k, and n). Overgrowths of MGSC result in a regular outer surface (e.g. Fig. 3a) as compared to the irregular bladed surfaces (Fig. 3b) of intermediate calcite. MGSC forms layers of variable thickness. Small, discontinuous, "golf-tee" shaped overgrowths can form on the tips of bladed calcite (Fig. 8h; see Whelan et al., 1996) or MGSC can comprise entire secondary mineral crusts (Fig. 8k). MGSC contains only liquid-only fluid inclusions indicating formation at low temperatures (Wilson et al., 2002). Opal layers can be numerous and locally continuous or discontinuous (Figs. 8i and j). Most importantly, MGSC provides a chemically distinct fingerprint that is paragenetically consistent, and which can be traced across Yucca Mountain allowing the histories of secondary minerals across the site to be linked.

7.2. Paragenesis of Fractures and Breccias

Fracture occurrences predominate in the NPR, SPR and the IFZ and the following paragenesis is compiled from samples within these three areas. The wall rock surface in most fracture and breccia samples consists of broken tuff that lacks vapor-phase minerals. These surfaces suggest that fracture/breccia development occurred after vapor-phase alteration of the host tuffs and, in

turn, indicate that secondary minerals in fractures and breccias began to precipitate later than secondary minerals in LC.

Layered calcite in fractures and breccias consists of multiple planar calcite layers defined by small tuff inclusions. Layered calcite, basal calcite, and fluorite precipitated around wall rock in the IFZ (Figs. 4g and h) and chalcedony-quartz-brown opal-fluorite was deposited in the NPR and SPR (Fig. 4; Fig. 8l). Chalcedony-quartz-brown opal is probably not present in the IFZ because silica deposition pre-dated the fracturing event. If this interpretation is correct, IFZ fluorite is younger than fluorite associated with chalcedony-quartz-brown opal in the NPR and SPR. Geochronology, fluid inclusion petrography, and microthermometry (Wilson et al., 2002) support these interpretations.

Chalcedony-quartz-brown opal-fluorite in fracture occurrences commonly forms multiple layers. These layers are different from the single layers of silica minerals in LC samples that contain less fluorite. In these fracture samples, sparse two-phase fluid inclusions have been observed in both quartz and fluorite growing around the host tuffs (Wilson et al., 2002).

Clearer calcite typically precipitated on the early, basal minerals described above (Fig. 8m). Calcite that precipitated on layered basal calcite in the IFZ is usually clear and exhibits strong orange luminescence. In these samples, this clear calcite comprises the majority of the crusts and later overgrowths are not generally present. Large bladed calcite crystals are uncommon in fracture occurrences; however, small blades are present in many samples where open space permitted crystal growth.

As in LC, the youngest calcite present in fractures and breccias is MGSC; however, it is more difficult to recognize than in LC (Fig. 4c). The growth zoning within MGSC is generally simpler in fracture and breccia samples and MGSC overgrowths are usually thin and discontinuous (Fig. 8i). However, in some fracture and breccia localities in the NPR and SPR, MGSC growth zoning is well developed and the layer is locally thick, complex, and continuous (Figs. 6 and 8n). MGSC in fractures and breccias contains concentrations of Mg (~1 wt. %) similar to those in LC, and is petrographically and geochemically equivalent to MGSC identified in LC. In some fracture samples that contained abundant open space, MGSC overgrowths occur on the outer surface, and also line inner pore spaces (e.g. sample ESF 78+05.2). Textures indicate that the MGSC is a late-stage overgrowth in these pores and is temporally related to the outer overgrowths.

8. DISCUSSION

8.1. Mineral correlation

MGSC is the single, chemically distinctive mineral layer that can be correlated across the site. Textural relationships and chemical data show that MGSC or intergrown associated opal precipitated last in the paragenetic sequence. Intergrown opal has been dated using U-Pb techniques and results indicate that MGSC began precipitating between 2.9 – 1.9 Ma and has continued to precipitate to within the past few thousands of years (Wilson et al., 2002).

Bladed calcite, which is present in a large number of samples, probably reflects precipitation over an extended period of time, or during discrete intervals over time. This calcite does not have a distinctive chemical composition or luminescence. C and O isotopic signatures of bladed calcite (Fig. 7) exhibit a broad range, consistent with precipitation over extended time.

Furthermore, fluid inclusion petrography has shown that early bladed calcite contains rare two-phase fluid inclusions, and only liquid-only fluid inclusions are present in later bladed calcite (Wilson et al., 2002).

Chalcedony-quartz-brown opal is present in LC and in some fracture and breccia samples. U-Pb dating indicates that the chalcedony precipitated between 4 – 9 Ma (Wilson et al., 2002), consistent with the "early to intermediate" paragenetic position determined for this layer by petrography. These ages indicate that all chalcedony in the silica layer did not form at the same time and the silica layer does not represent a time line that can be correlated across the site.

8.2. C and O isotope Data

A comparison of the isotopic data shown in Figure 7 with data from Whelan et al. (in press) shows that similar ranges of C and O isotopic signatures and trends of increasing $\delta^{18}O$ and decreasing $\delta^{13}C$ with respect to decreasing age were determined by both studies. These results show that careful micro sampling of calcite in growth zones within a well-constrained paragenetic sequence does not produce unique isotopic signatures for calcite of different ages and habits. The lack of unique signatures for secondary mineral layers is most clearly demonstrated by MGSC, which has isotopic compositions that overlap with compositions determined for paragenetically older calcite.

Current results parallel results reported by Whelan et al. (in press) and indicate that calcite precipitated from meteoric fluids as interpreted by Whelan et al. (in press). The interpretation that some early calcite formed from ~ 50 – 80 °C fluids (Paces et al., 1997) is consistent with the microthermometry data of Wilson et al. (2002). Finally, a meteoric fluid source is further indicated by low δD compositions of inclusion fluids from intermediate calcite and MGSC (Wilson et al., 2002).

8.3. Significance of Mg-enriched Growth-zoned Sparry Calcite

The presence of PMC and MGSC indicate that Mg was available and was incorporated into the calcite structure during two periods of calcite deposition. It is generally accepted that the Mg concentrations in calcite are positively correlated with elevated temperatures and elevated Mg/Ca ratios of the source fluid (e.g. Scoffin, 1987). Wilson et al. (2002) showed that some early calcite contains primary fluid inclusions indicating calcite deposition at temperatures of 35 – 85 °C; such elevated temperatures could explain the incorporation of Mg into early calcite around tridymite. However, the majority of calcite that precipitated at elevated temperatures does not exhibit Mg-enriched growth zoning. Furthermore, MGSC contains rare liquid-only fluid inclusions indicating formation from low temperature fluids (Wilson et al., 2002). Therefore, it is unlikely that temperature controlled the Mg composition of the calcite. Instead, Mg-enrichment is likely controlled by the Mg/Ca ratio of the fluid, and early fluids that precipitated PMC and late fluids that precipitated MGSC probably contained higher Mg/Ca than fluids from which most of the calcite precipitated.

The irreversible change in the deposition of calcite with growth zones of alternating Mg-enriched and Mg-free calcite during the last few million years reflects a permanent change in the fluids that accessed Yucca Mountain. The fine oscillatory growth zoning shows that the Mg/Ca ratio in the fluid fluctuated repeatedly and in a fairly regular, cyclical manner. However the source of the Mg and reason for this change in deposition of calcite type are less clear.

The consistent presence and oscillatory nature of the growth zones suggest that they may be recording fluctuations related to changes in climate from around 2.9 Ma to the present day (Wilson et al., 2002). This time period corresponds with a major change in Northern Hemisphere glaciation which occurred around 2.67 Ma (Prueher and Rea, 1998). An abrupt change in deep-sea sediment character related to a change from a non-glacial to a glacial environment occurred across the North Pacific at this time. This change occurred too rapidly to be a direct response to tectonic or orbital forcing (Prueher and Rea, 1998) and terrestrial changes that corresponded with deep sea-related changes would be expected. The gradual uplift of the Sierra Nevada, west of Yucca Mountain, caused a change in the water chemistry during the last 3 m.y. (Smith et al., 1983). This change in chemistry led to deposition of considerable dolomite and Mg-enriched clays in playas and lakes in the Amargosa desert during the Pliocene (3.2 - 2.1 Ma) (Hay et al., 1986). These minerals may have contributed Mg to fluids that percolated into Yucca Mountain during climate-related cycles, forming MGSC. This process may have been accelerated by the earlier Pliocene nonglacial environment, when the climate was substantially wetter and springs in the Amargosa Desert were more widespread and had greater discharge (Hay et al., 1986). Alternatively, it is possible that the increase in Mg could be related to atmospheric dusts related to erosion of Paleozoic dolomites in the southwest (*J. Stuckless, personal communication, 2000*).

The fine and complex growth zones are not continuous across a thin section suggesting that the larger calcite crystals formed by the constructive deposition of numerous small overgrowths. These discontinuities are small-scale versions of discontinuous MGSC present in numerous samples and illustrated in Figure 8. These discontinuities are not consistent with saturation of the site by aqueous fluids.

8.4. Variability of Secondary Minerals

The distribution of secondary minerals within the site indicates that processes responsible for their formation were dominantly controlled by the amount of fluid that infiltrated the volcanic rocks, the porosity and permeability of the depositional sites, and the temperature and trace element chemistry of the fluids. All of these variables probably changed through time. In general most of the host rocks, except where they are highly welded, are relatively porous and permeable (Whelan et al., in press). However, local porosity and permeability would change as secondary minerals precipitated and closed some fluid pathways. This could result in early mineral precipitation in some localities and later mineral precipitation in other sites. Some variations in the mineral record can be explained by varying fluid compositions and temperatures through time (Wilson et al., 2002). The presence of abundant silica minerals in the NPR and the absence of these minerals in the IFZ are probably related to the presence of early fluids with elevated temperatures and saturated in silica in the NPR, prior to formation of fractures in the IFZ.

An important variable controlling the distribution and abundance of secondary minerals at Yucca Mountain is probably the amount of aqueous fluid that infiltrated the site. Approximately 90 % of the open space at Yucca Mountain contains no secondary minerals or any record of fluid influx. Calculations of the abundance of secondary minerals along 30-m sections at 100 m intervals over the entire ESF showed that < 6 % of fractures greater than 1 m long contain mineral coatings (Whelan et al., in press). Mapping of LC over five 30 m sections indicated that between 1 – 42 % contained secondary minerals and the majority of cavities lacked any secondary mineral record (Whelan et al., in press). Secondary minerals that may have begun to precipitate more than 12 million years ago following deposition of the tuff rarely form

crusts more than a couple centimeters in thickness and, where present, are typically millimeters to less than a centimeter thick. This mineral record contrasts strongly with the sequence of calcite that precipitated at Devils Hole, Nevada under saturated conditions (Winograd et al., 1992). Devils Hole calcite precipitated at an average rate of 0.7 mm/1000 years (Ludwig et al., 1992) producing a thick layer of vein calcite more than 0.3 m thick in 500,000 years (Winograd et al., 1992). The sparse and thin secondary mineral record at Yucca Mountain argues strongly that aqueous fluids did not access most open space at Yucca Mountain or saturate the site in the past. The Yucca Mountain mineral record is, instead, consistent with formation in a vadose environment.

Input from a fluid with a consistent composition at constant temperature over time would produce a consistent secondary mineral record in depositional sites accessed by the fluids. Such a depositional record is exhibited by MGSC, which has been precipitating for the past 1.9 –2.9 Ma (Wilson et al., 2002). Although the majority of open spaces do not contain this material, MGSC is distributed across Yucca Mountain, which suggests that there are preferred fluid pathways through the UZ.

8.5. Formation of Secondary Minerals in the Vadose Zone

The question of whether the secondary minerals formed in a vadose or phreatic environment cannot be directly answered, because no single texture observed in the rocks unequivocally identifies the environment of precipitation. This may simply be due to the limited fluid infiltration of the site. However, there are a number of observations that are not consistent with the formation of secondary minerals in the phreatic zone.

First, as discussed above, the majority of primary and secondary porosity contains no evidence of secondary minerals. If secondary minerals precipitated in a phreatic environment by upwelling hydrothermal fluids (Dublyansky, 1998; Dublyansky et al., 2001) or rising ground water (Szymanski, 1987, 1989), a more extensive record of secondary minerals would be expected in the available open space.

Second, some pores in LC, fractures, and breccias are rimmed by thin layers of calcite, suggestive of meniscus textures (e.g. Fig. 3; sample ESF 21+61.8) that indicate precipitation in a vadose environment (James and Choquette, 1990). Some pore fillings exhibit multiple luminescent growth zones under CL indicating multiple fluid events.

Third, the lack of isopachous textures at Yucca Mountain is not consistent with formation in the phreatic zone (James and Choquette, 1990). Our observations are in agreement with observations by USGS scientists (Whelan et al., 1996) that secondary minerals occur predominantly on the footwalls and bases of LC, fractures, and breccias, consistent with precipitation in the vadose zone.

Fourth, detailed growth zoning of MGSC indicates that repeated fluctuations in fluid composition are required to account for the Mg-enriched and depleted growth zoning. Such fluctuations are difficult to reconcile with a saturated environment. The discontinuous nature of the growth zones is consistent with addition of small amounts of fluid with fluctuating Mg concentrations.

Fifth, if upwelling hydrothermal fluids periodically invaded Yucca Mountain, the fluids would be cooled by contact with the colder rocks, and silica minerals, particularly quartz, would precipitate. Although silica minerals are relatively abundant in some samples in the NPR and

SPR, these minerals are part of the early to intermediate assemblages, and silica minerals are sparse in younger assemblages and in other parts of the site.

Sixth, no single location or sample records the entire history of secondary mineralization, suggesting that whatever process was responsible for deposition did not occur uniformly throughout the repository horizon. Such a record is difficult to reconcile with a phreatic environment, but is consistent with mineral precipitation in a vadose zone.

Finally, the presence of glass in the host tuffs suggest that these tuffs have not been below the static water level (Levy, 1991). These data strongly indicate that the volcanic rocks have not been in contact with fluids in a phreatic environment for any length of time during their history.

The above observations argue strongly for precipitation of secondary minerals within a vadose environment. The lack of any features that are typical of a phreatic environment make genetic models involving flooding of the repository by hydrothermal fluids or groundwater untenable. This study, alternatively, indicates that the most reasonable source of fluids responsible for secondary minerals is surficial waters that percolated into the mountain.

9. CONCLUSIONS

Detailed petrographic study of 155 samples collected from localities across the Yucca Mountain site allowed the construction of a paragenetic sequence based on extensive petrography integrated with trace element, isotopic, CL, and LA-ICP-MS analyses. The main conclusions from this study are summarized below.

1. Extensive petrography, paragenetic studies, and microprobe mapping indicate that early secondary minerals were heterogeneously distributed across the site. These early minerals consist of variable amounts of calcite, which is the most abundant mineral in the crusts, and lesser variable opal, chalcedony, fluorite, and quartz. Intermediate minerals consist of primarily calcite, often in distinctive bladed habits, with minor opal, chalcedony and quartz. These minerals contain no diagnostic trace element variations. The latest secondary minerals deposited across the site consist of sparry calcite and minor intergrown opal. This outermost calcite is chemically distinct, contains oscillatory Mg-enriched and depleted growth zones, is associated and intergrown with clear opal, and forms the youngest mineral layer that precipitated across the site. Petrographic studies indicated that secondary mineral crusts at most sample sites recorded an incomplete history of secondary mineral precipitation. Some samples contain only early, intermediate, or late minerals, and few samples exhibit a complete early to late sequence.

2. The youngest secondary minerals that precipitated were Mg-enriched growth zoned sparry calcite (MGSC) and intergrown opal. MGSC occurs in > 65 % of the samples and, with or without associated opal, is always the paragenetically youngest mineral. MGSC has a consistent texture and unique chemical signature, can be correlated across the site in LC, fracture, and breccia occurrences, and links the history of secondary mineral deposition at sample sites across Yucca Mountain. This allows construction of a mineral paragenesis that is representative of secondary minerals across the site and provides a basis for subsequent fluid inclusion and geochronology studies that constrain the time-temperature history of fluid flux through the site.

3. The textures and features of the secondary minerals in the unsaturated zone at Yucca Mountain are not consistent with saturation of the site by aqueous fluids and mineral formation in the phreatic environment, but are consistent with precipitation of secondary minerals in the vadose environment from surficial meteoric fluids. Outermost MGSC formed from the infiltration of small amounts of aqueous fluid. The oscillatory nature of the Mg growth zoning may be related to variations in climate during the last 3 Ma.

Acknowledgements. We would like to thank Joel Rotert, Drew Coleman, and Joe Whelan for their assistance during sample collection. Special thanks go to Mark Mercer (Petrographics, Montrose, CO) for making the spectacular polished sections, and to Bob Bodnar for his technical review of this report. Bob Bodnar, Yuri Dublyanski, Bob Goldstein, Ed Roedder, Joe Whelan and Ike Winograd are thanked for discussions on all aspects of this project. We thank the following for their technical assistance: Sarah Lundberg (UNLV, EPMA), Luis Gonzalez and Scott Carpenter (University of Iowa, stable isotopes), and Paul Lechler (Nevada Bureau of Mines, LA-ICP-MS). Funding for this study was awarded to JSC under DOE Cooperative Agreement DE-FC08-98NV-12081.

All data presented in this paper were collected under the UCCSN Quality Assurance program. Technical Data Managment System data tracking number UN0203SPA004JC.001 correlates to data collected during this study. Access to electronic data was limited to task personnel and controlled with the use of passwords. Loss was prevented by use of backup files. Manual entry and file transfers were verified for accuracy. No electronic data were lost or corrupted.

REFERENCES

Bish D. L. (1989) Evaluation of past and future alterations in tuff at Yucca Mountain, Nevada, based on the clay mineralogy of drill cores USW G-1, G-2, and G-3. Los Alamos National Laboratory Report LA-10667-MS.

Bish D. L. and Chipera S. J. (1989) Revised mineralogic summary of Yucca Mountain, Nevada. Los Alamos Nat. Lab. Rept. LA-11497-MS.

Buesch D. C., Spengler R. W., Moyer T. C. and Geslin J. K. (1996) Proposed stratigraphic nomenclature and macroscopic identification of lithostratigraphic units of the Paintbrush Group exposed at Yucca Mountain, Nevada. U. S. Geological Survey Open-File Report.

Caporusico F., Vaniman D., Bish D., Broxton D., Arney B., Heiken G., Byers F., Gooley R. and Semarge E. (1982) Petrographic studies of drill cores USW G-2 and UE25b-1H, Yucca Mountain, Nevada. Los Alamos National Laboratory Report LA-10927-MS.

Carlos B. A. (1994) Field guide to fracture-lining minerals at Yucca Mountain. Los Alamos National Lab. Rep. LA-12803-MS.

Christiansen R. L, Lipman P. W., Carr W. J., Byers F. M Jr., Orkild P. P. and Sargent K. A. (1977) Timber Mountain-Oasis Valley caldera complex of southern Nevada. *GSA Bulletin* **88**, 943-959.

Coplen T. B., Kendall C. and Hopple J. (1983) Comparison of stable isotope reference samples. *Nature* **302**, 236-238.

Data Tracking Number UN0203SPA004JC.001. Thermochronological evolution of calcite formation at Yucca Mountain. Submittal date: 03/26/2002.

Day W. C., Dickerson R. P., Potter C. J., Sweetkind D. S., San Juan, C. A., Drake R. M and Fridrich C. J. (1998) Bedrock geologic map of the Yucca Mountain area, Nye County, Nevada. *Geologic Investigations Series* - U. S. Geol. Survey. pp. 21, 1 sheet.

Denniston R. F., Shearer C. K., Layne G. D. and Vaniman D. T. (1997) SIMS analyses of minor and trace element distributions in fracture calcite from Yucca Mountain, Nevada, USA. *Geochim. Cosmochim. Acta* **61**, 1803-1818.

Dublyansky Y. (1998) Fluid inclusion studies of samples from the Exploratory Study Facility, Yucca Mountain, Nevada. Institute for Energy and Environmental Research Report, Washington.

Dublyansky Y., Szymanski J., Chepizhko A., Lapin B. and Reutsky V. (1998) Geological history of Yucca Mountain (Nevada) and the problem of a high-level nuclear waste repository. In *Defense Nuclear Waste Disposal in Russia* (eds. M. Stenhouse and V. Kirko). NATO Series, Kluwer Academic Publishing, Netherlands, pp. 279-292.

Dublyansky Y., Ford D. and Reutski V. (2001) Traces of epigenetic hydrothermal activity at Yucca Mountain, Nevada: preliminary data on the fluid inclusion and stable isotope evidence. *Chemical Geology* **173**, 125-149.

Hay R. L., Pexton R. E., Teague T. T. and Kyser T. K. (1986) Spring-related carbonate rocks, Mg clays, and associated minerals in Pliocene deposits of the Amargosa Desert, Nevada and California. *GSA Bulletin* **97**, 1488-1503.

Heizler M. T., Perry F. V., Crowe B. M., Peters L. and Appelt R. (1999) The age of the Lathrop Wells volcanic center: an $^{40}Ar/^{39}Ar$ dating investigation. *Jour. Geophy. Res.* **104**, 767-804.

James, N.P. and Choquette, P.W. (1990) Limestones - the meteoric diagenetic environment. In Diagenesis (eds. I.A. McIlreath, and D.W. Morrow). Geoscience Canada Reprint Series

4, p. 35-73.

Levy S. (1991) Mineralogic Alteration History and Paleohydrology at Yucca Mountain, Nevada, High Level Radioactive Waste Management, *Proc. Conf. High Level Rad. Waste Mgmt.*, 477-485.

Levy S. S., Norman D. I. and Chipera S. J. (1996) Alteration history studies in the Exploratory Studies Facility, Yucca Mountain, Nevada, USA. *Proceedings of the Materials Research Society*, 412-790.

Ludwig K. R., Simmons K. R., Szabo B. J., Winograd I. J., Landwehr J. M., Riggs A. C. and Hoffman R. J. (1992) Mass-spectrometric ^{230}Th-^{234}U-^{238}U dating of the Devils Hole calcite vein. *Science* **258**, 284-287.

Machel H. G., Mason R. A., Mariano A. N. and Mucci A. (1991) Causes and emission of luminescence in calcite and dolomite. In *Luminescence Microscopy and Spectroscopy – Qualitative and quantitative applications* (eds. C. E. Barker and O. C. Kopp). Society for Sedimentary Geology, Short course 25, pp. 9-25.

Mongano G. S., Singleton W. L., Moyer T. C., Beason S. C., Eatman G. L. W., Albin A. L. and Lung R.C. (1999) Geology of the ECRB Cross Drift - Exploratory Studies Facility, Yucca Mountain Project, Yucca Mountain, Nevada. U.S. Department Of Energy.

Paces J. B., Neymark L. A., Marshall B. D., Whelan J. F. and Peterman Z. E. (1996) Ages and origins of subsurface secondary minerals in the exploratory studies facility (ESF). U.S. Geological Survey – Yucca Mountain Project Branch, Milestone report 3GQH450M.

Paces J. B., Marshall. B. D., Whelan, J. F. and Neymark L. A. (1997) Progress Report on Unsaturated Zone Stable and Radiogenic Isotope Studies, U.S. Geological Survey Milestone report SPC23FM4.

Paces J. B., Neymark, L. A., Marshall, B. D., Whelan J. F. and Peterman Z. E. (2001) Ages and origins of calcite and opal in the Exploratory Studies Facility Tunnel, Yucca Mountain, Nevada. U.S. Geological Survey, Water-Resources Investigations Report 01-4049.

Prueher L. M. and Rea D. K. (1998) Rapid onset of glacial conditions in the subartic North Pacific region at 2.67 Ma: Clues to causality. *Geology* **26**, 1027-1030.

Sawyer D. A., Fleck R. J., Lanphere M. A., Warren R. G., Broxton D. E. and Hudson M. R. (1994) Episodic Caldera Volcanism in the Miocene Southwestern Nevada Volcanic Field: Revised Stratigraphic Framework, $^{40}Ar/^{39}Ar$ Geochronology, and Implications for Magmatism and Extension. *GSA Bulletin* **106**, 1304-1318.

Scoffin T. P. (1987) *An introduction to carbonate sediments and rocks*, Blackie and Son Ltd., Glasgow.

Smith G. L., Barczak V. J., Moulton G. and Liddicoat J. C. (1983) Core KM-3, a surface to bedrock record of late Cenozoic sedimentation in Searles Valley, California: U.S. Geological Survey Prof. Paper 1256.

Stewart J. H. (1988) Tectonics of the Walker Lane Belt, Western Great Basin – Mesozoic and Cenozoic Deformation in a Zone of Shear. In *Metamorphism and crustal evolution of the western United States* (ed. W. G. Ernst), Vol. VII, Prentice-Hall Inc., New Jersey, pp. 684-713.

Stuckless J. S. and Dudley W. W. (2001) The Geohydrologic Setting of Yucca Mountain, Nevada. *Applied Geochemistry, in press.*

Szymanski J. S. (1987) Conceptual considerations of the Death Valley Groundwater System with Special Emphasis on the Adequacy of this System to Accommodate the High-Level

Nuclear Waste Repository (Draft). DOE internal report, Yucca Mountain Project Office, Las Vegas Nevada.

Szymanski J. S. (1989) Conceptual considerations of the Yucca Mountain Groundwater System with Special Emphasis on the Adequacy of this System to Accommodate the High-Level Nuclear Waste Repository. DOE internal report, Yucca Mountain Project Office, Las Vegas Nevada.

U.S. Department of Energy (1988) Site characterization plan, Yucca Mountain site, Nevada research and development area, Nevada. U.S. Dept. Energy Report, DOE/RW-0199-8 Volumes.

Vaniman D. T. (1993) Calcite deposits in fractures at Yucca Mountain, Nevada. *Proc. 4th Intl. Conf. High level Rad. Waste Mgmt.*, 1935-1939.

Vaniman D. T. (1994) Calcite deposits in drill cores USW G-2 and USW GU-3/G-3 at Yucca Mountain, Nevada. Los Alamos National Lab. Rept. LA-12720-MS.

Vaniman D. T. and Chipera S. J. (1996) Paleo-transport of lanthanides and strontium recorded in calcite compositions from tuffs at Yucca Mountain, Nevada. *Geochim. Cosmochim. Acta* **60**, 4417-4433.

Whelan J. F. and Moscati R. J. (1998) 9 m.y. record of southern Nevada climate from Yucca Mountain secondary minerals. *Proc. Eighth Conf. High Level Rad. Waste Mgmt.*, 12-15.

Whelan J. F., Vaniman D. T., Stuckless J. S. and Moscati R. J. (1994) Paleoclimatic and paleohydrologic records from secondary calcite: Yucca Mountain, NV. *Proc. Conf. High Level Rad. Waste Mgmt.*, 2738-2745.

Whelan J. F., Moscati R. J., Allerton S. B. M. and Marshall. B. D. (1996) Applications of isotope geochemistry to the reconstruction of Yucca Mountain, Nevada, Paleohydrology – status of investigations. U.S. Geological Survey, Open-file report 98-83.

Whelan J. F., Moscati R. J., Allerton S. B. M. and Marshall. B. D. (1998) Applications of isotope geochemistry to the reconstruction of Yucca Mountain, Nevada, Paleohydrology – status of investigations. U.S. Geological Survey, Open-file report.

Whelan J. F., Paces J. B., Neymark L. A. and Peterman, Z. E. (2000) Thermochronology of fluid inclusions in Secondary Calcite from the Unsaturated Zone at Yucca Mountain, Nevada. U.S. Geological Survey Fiscal Year 2000 Status Report.

Whelan J. F., Roedder E. and Paces J. B. (2001) Evidence for an unsaturated-zone origin of secondary minerals in Yucca Mountain, Nevada, *Proc. Conf. High Level Rad. Waste Mgmt.*, N1.

Whelan J. F., Paces J. B. and Peterman Z. E. Paragenetic Relations and Evidence for Secondary Mineral Formation in Unsaturated-zone Tuffs at Yucca Mountain, Nevada. *Applied Geochemistry, (in press)*.

Wilson N. S. F., Cline J. S. and Amelin Y. (2002) Thermochronological Evolution of Calcite Formation at the Potential Yucca Mountain Repository Site, Nevada: Part 2, Fluid Inclusion Analyses and U-Pb Dating, *Companion report submitted to DOE.*

Winograd I. J. (1981) Radioactive waste disposal in thick unsaturated zones. *Science* **212**, 1457-1464.

Winograd I. J., Coplen T. B., Landwehr J. M., Riggs A. C., Ludwig K. R., Szabo B. J., Kolesar P. T. and Revesz K. M. (1992) Continuous 500,000-year climate record from vein calcite in Devils Hole, Nevada. *Science* **258**, 255-260.

FIGURE AND TABLE CAPTIONS

Fig. 1 Simplified location and geological map and cross section of Yucca Mountain, Nevada (adapted from Day et al., 1998 and Paces et al., 2000). Cross section shows the underground location of the potential repository. Stratigraphic units are after Buesch et al. (1996). Approximate locations of the water table, unsaturated zone and saturated zone are also shown.

Fig. 2 Location of samples collected from the Exploratory Studies Facility (ESF), ECRB Cross Drift (ECRB), and exploratory alcoves. Unfilled circles indicate samples from a LC, whereas filled circles indicate samples from a fracture or breccia occurrence. To simplify discussion in the text the site has been divided into the following zones; North portal and ramp (NPR), Lithophysal Cavity Zone (LCZ), Intensely Fractured Zone (IFZ), South Portal and Ramp (SPR), and ECRB Cross Drift (ECRB).

Fig. 3 Images of standard polished sections (~ 3.5 cm wide) illustrating the variation of open space secondary minerals in LC (A – C), fractures (D – F), and breccias (G – I). Arrows in the lower left corners indicate the growth direction of secondary minerals. Sample ESF 48+11 **(D)** contains multiple slices of a thin mineral crust; in all cases the crusts precipitated towards the top of the section. Sample ECRB 12+90 **(G)** contains two sections of the mineral crust mounted on the same slide. The bases of the crusts are at the top and bottom of the section. The white arrows in **(H)** highlight thin layers of calcite that rim open pores and are suggestive of meniscus textures commonly found in the vadose zone. Abundant open spaced is preserved in all LC, fracture, and breccia occurrences. (Cdy = Chalcedony, Qtz = Quartz, C = Calcite, O = Opal)

Fig. 4 Composite photomicrographs illustrating mineral and textural relationships in secondary mineral crusts. The large arrows indicate the growth direction of the mineral crusts. Photomicrographs were taken in plane-polarized light (PPL), crossed polarized light (XPL), or partially crossed polarized light (PXPL). All sections were 100 μm thick resulting in higher order interference colors. The dashed white lines mark the boundary between MGSC and earlier minerals. **(A)** Photomicrograph in PPL of finer-grained calcite at the base of a LC, overgrowing tridymite (T) and being overgrown by bladed calcite (slender crystals) in the LCZ. Early bladed calcite consists of smaller slender blades on the scale of a few millimeters while later calcite blades are longer. **(B)** Early blocky, dark calcite in PPL that encompasses vapor-phase tridymite (T) and tuff pieces at the base of a LC. **(C)** Bladed calcite (PXPL) overgrown by MGSC and opal at the outer edge of a LC crust. The white arrows indicate growth zones in MGSC. Note that opal is concordant (opal layers) and discordant (outer opal) with respect to the growth zoning. **(D)** Fracture sample from the NPR in PPL containing tridymite (T), overlain by chalcedony, and then, in turn, by brown opal and MGSC. **(E)** Photomicrograph (PPL) of opal layers and hemispheres within MGSC from a LC crust. Opal hemispheres highlight previous depositional surfaces. MGSC and opal overgrew earlier 'nail head' calcite (see Fig. 5C). **(F)** Chalcedony layer (XPL) within a calcite crust from a LC. Vapor-phase tridymite (T) is overgrown by basal calcite and some dissolution of this calcite was followed by precipitation of chalcedony. Chalcedony is overgrown by clear, bladed

calcite that is in turn, overgrown by MGSC. (G) Layered calcite (PPL) at the contact of the secondary minerals with the wall rock from a fracture occurrence in the IFZ. **(H)** Fracture / breccia sample (PPL) from the IFZ containing fluorite growing around the host tuff and overlain by a number of generations of calcite. The layered calcite, which occurs adjacent to the wall rock in G occurs within open space fillings and is overgrown by later secondary minerals. This indicates that older material fell into the breccia and was cemented by younger minerals. Outer non-descript calcite overgrows the host rock and is the youngest secondary mineral in the sample. This section shows that paragenetically early material, including fluorite and host tuff, can be spatially but not temporally related to paragenetically late minerals. **(I)** Fracture sample (PXPL) from the NPR containing calcite (Cal) replaced by chalcedony. White arrows indicate anhedral calcite remnants in the chalcedony and black arrows highlight an early calcite cleavage pseudomorphed by chalcedony. Chalcedony contains inclusions of fluorite and is overgrown by quartz, which in turn is overgrown by MGSC and brownish opal (O). **(J)** Chalcedony-brown opal-quartz layers (XPL) in a LC crust. Chalcedony occurs as a number of discrete layers and commonly contains euhedral quartz crystals on the outermost edges of the growths. **(K)** Quartz (PPL) at the basal part of a fracture crust from the NPR containing small cubic crystals and nodules of fluorite (Fl). **(L)** Cathodoluminescence in basal calcite, from the IFZ, illustrating detailed oscillatory growth zoning. Growth zones are typically planar or rounded and approximately 50 μm thick. Truncated growth zoning highlights breaks in precipitation.

Fig. 5 Pairs of backscatter electron (BSE; left) images and Mg X-ray maps (right) illustrating the presence and absence of Mg in calcite. In the Mg maps the lighter color indicates higher concentrations of Mg. Quantitative analyses (in wt. %) for Mg are indicated on the maps. **(A)** Map from the basal part of a LC crust with vapor-phase tridymite overgrown by fluorite (Fl) and then by early calcite. Calcite growing around tridymite and fluorite contains patchy Mg-enriched calcite (PMC). Calcite from the center of the map does not contain detectable Mg. **(B)** Map of LC calcite crust (shown in Fig. 5F) from tridymite at the base outward to basal calcite and a chalcedony layer, to bladed calcite and MGSC (top). PMC occurs around the tridymite and adjacent to the wall rock and is not clearly related to crystal growth. The majority of the crust, including bladed calcite, does not contain detectable Mg. Bladed calcite is overgrown by MGSC containing clearly visible individual growth zones. Textures indicating dissolution of calcite at the base of the chalcedony are visible in the BSE image. **(C)** Map across a LC crust from basal calcite to outer MGSC. In BSE imaging irregular calcite at the base of the section is overgrown by clear calcite and then by MGSC associated with opal. Opal layers mark the boundary between basal and intermediate calcite and approximately mark the boundary between intermediate calcite and MGSC. The Mg map clearly shows that MGSC occurs only on the outermost part of the sample. The preexisting depositional surface for MGSC is indicated by the dashed white line and delineates the distinctive 'nail head' crystals. The dashed line also indicates that MGSC and intermediate calcite cannot be distinguished based on petrography alone, and that opal layers dated from within MGSC (see Wilson et al., 2002) formed after MGSC had began precipitating.

Fig. 6 Detailed X-ray map for Mg (up to 1 wt. %) illustrating the complex enriched and depleted Mg growth zoning present in MGSC (fracture sample ESF 78+41). Growth zones are locally discontinuous and cannot be traced across the sample. Bright spots are edge effects and do not represent high levels of Mg.

Fig. 7 Plot of $\delta^{13}C$ versus $\delta^{18}O$ for micro-milled calcite samples. Calcite samples are grouped according to calcite morphologies and/or paragenetic position in secondary mineral crusts. Filled symbols indicate samples that contained 2-phase fluid inclusions (see Wilson et al., 2002).

Fig. 8 Schematic illustration shows the paragenetic sequence of secondary minerals at Yucca Mountain. The left side of the figure represents fracture and breccia occurrences, and the right side illustrates LC crusts. Although there are significant differences, consistent mineral relationships are observed in LC and fracture and breccia occurrences. The figure illustrates the variable and heterogeneous nature of early secondary minerals, which contrasts significantly with the consistent presence of MGSC ± opal as the youngest, outermost minerals.

Table 1. C and O stable isotope data for calcite samples and calibration standards.

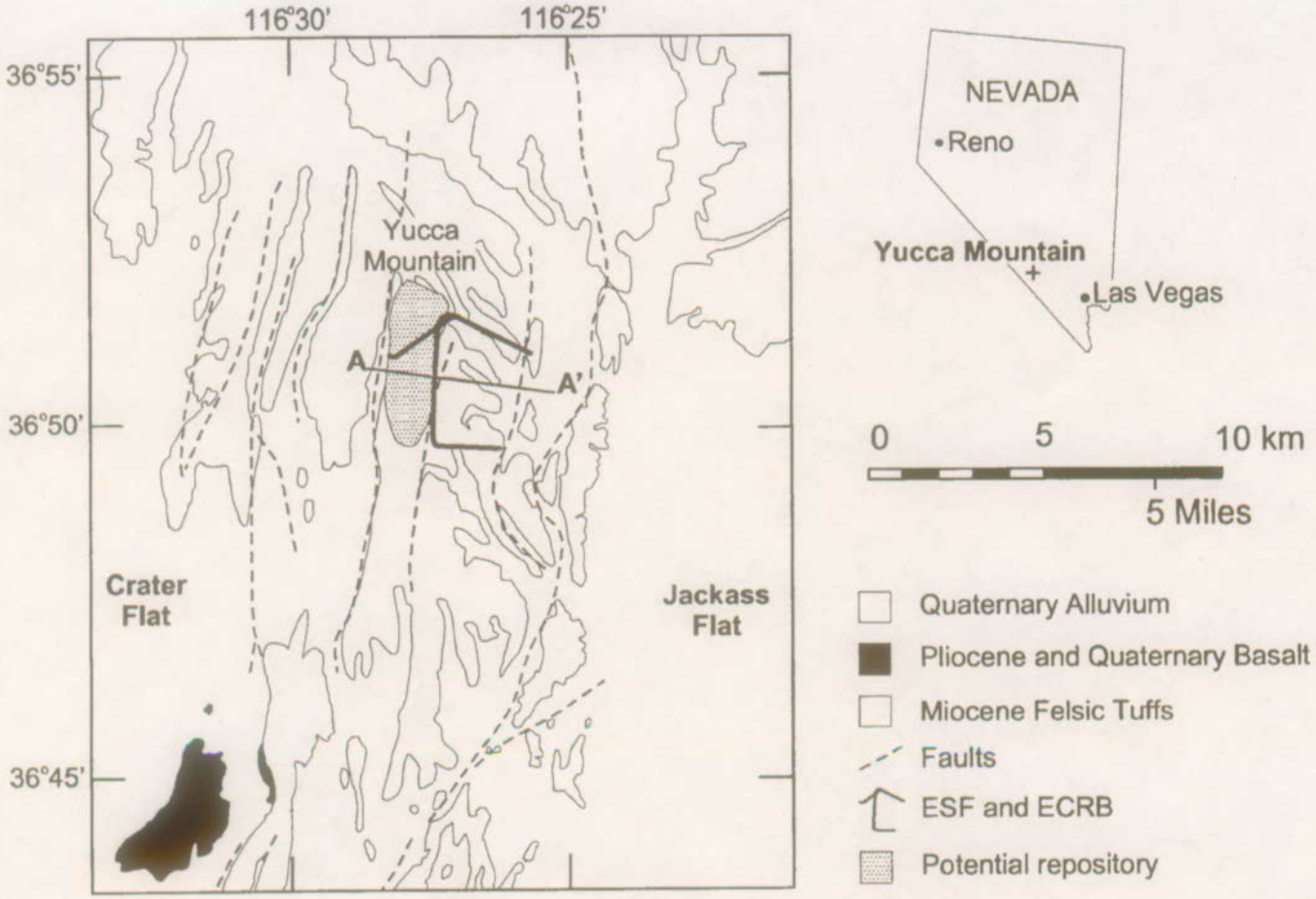
116°30'
116°25'
36°55'
36°50'
36°45'
Yucca Mountain
A
A'
Crater Flat
Jackass Flat
NEVADA
Reno
Yucca Mountain
Las Vegas
0
5
10 km
5 Miles
Quaternary Alluvium
Pliocene and Quaternary Basalt
Miocene Felsic Tuffs
Faults
ESF and ECRB
Potential repository

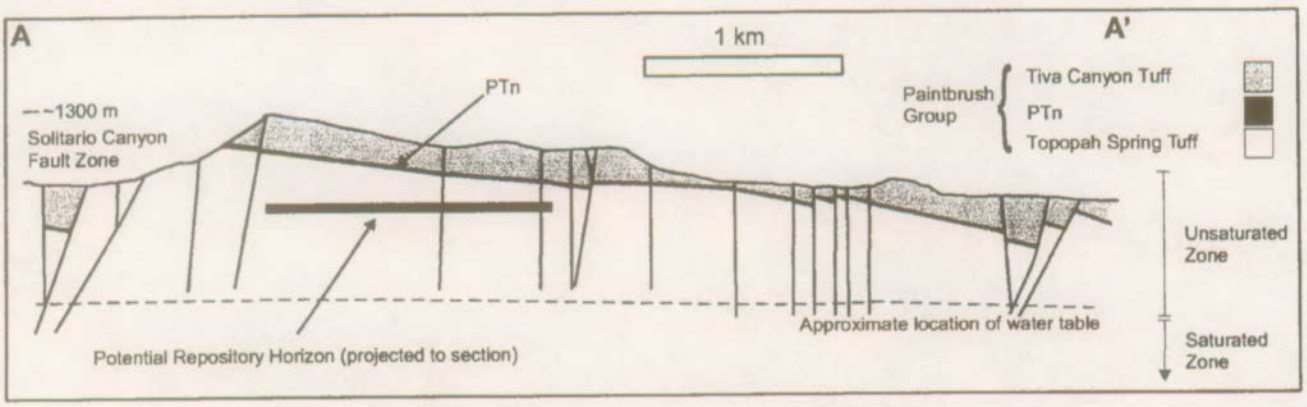
A
A'
1 km
~1300 m
Solitario Canyon Fault Zone
PTn
Paintbrush Group
Tiva Canyon Tuff
PTn
Topopah Spring Tuff
Unsaturated Zone
Saturated Zone
Approximate location of water table
Potential Repository Horizon (projected to section)

Figure 1

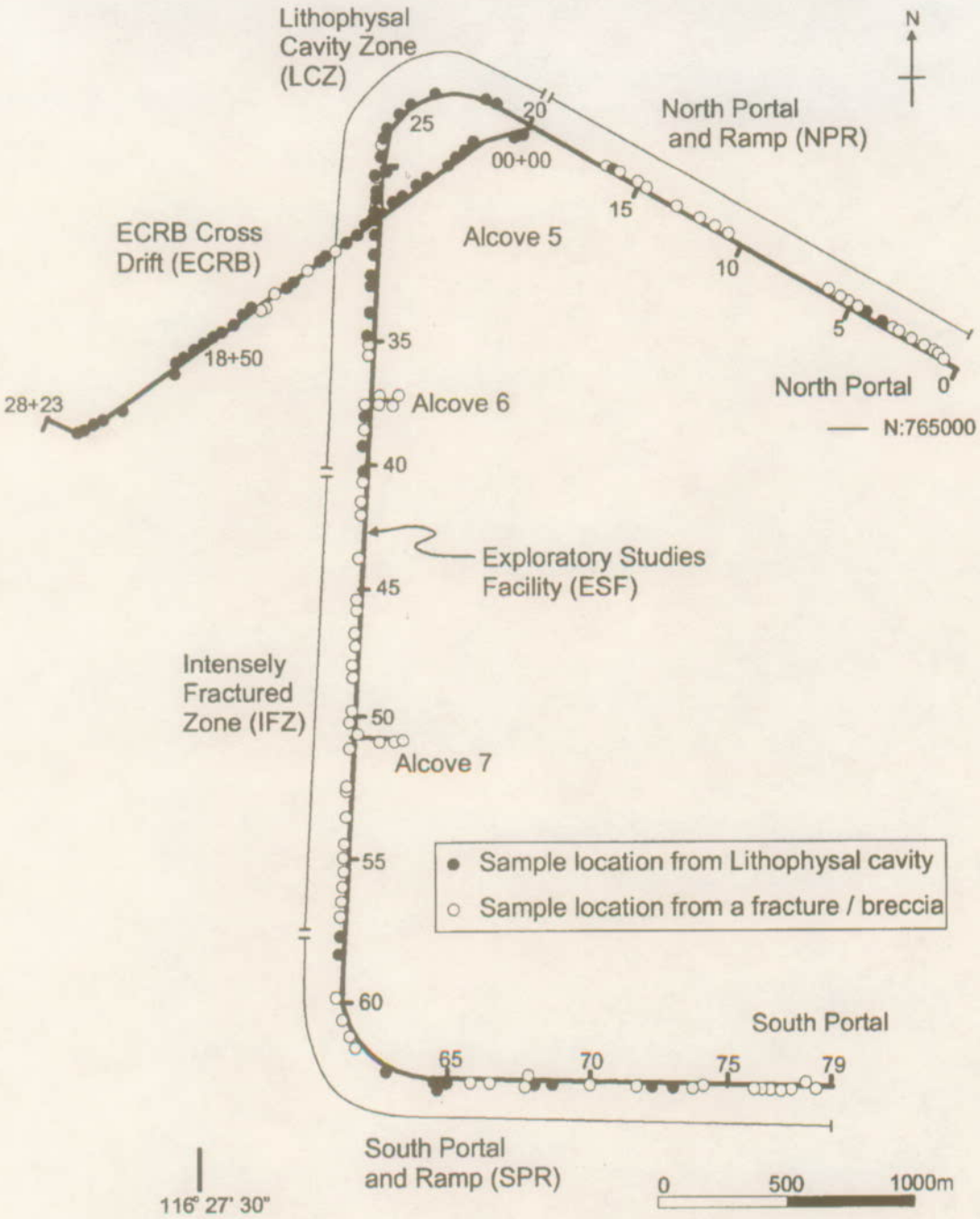
Lithophysal
Cavity Zone
(LCZ)
N
North Portal
and Ramp (NPR)
25
20
00+00
15
10
5
0
North Portal
N:765000
ECRB Cross
Drift (ECRB)
Alcove 5
18+50
28+23
35
Alcove 6
40
Exploratory Studies
Facility (ESF)
45
Intensely
Fractured
Zone (IFZ)
50
Alcove 7
55
Sample location from Lithophysal cavity
Sample location from a fracture / breccia
60
South Portal
65
70
75
79
South Portal
and Ramp (SPR)
0
500
1000m
116° 27' 30"

Figure 2

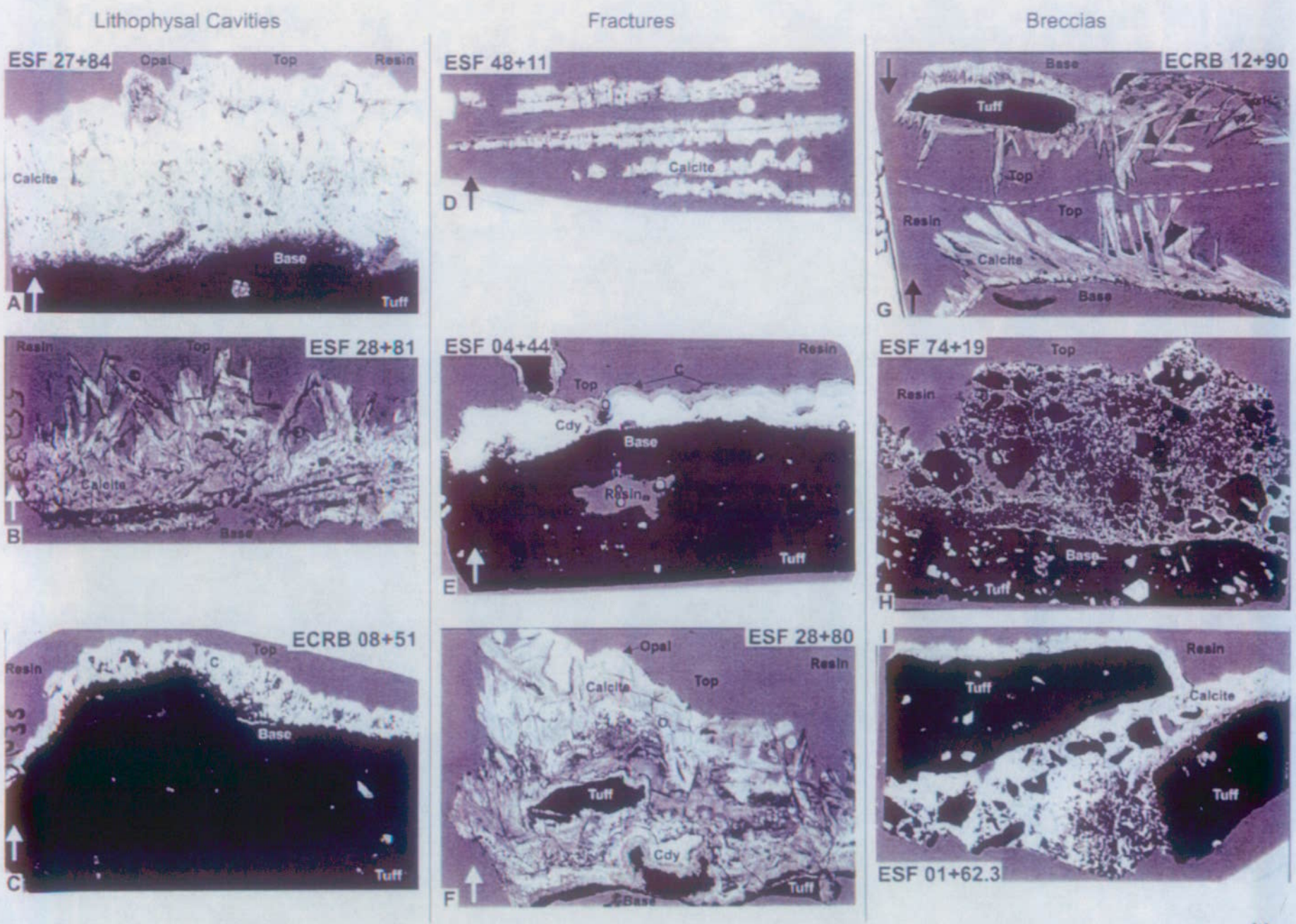
Lithophysal Cavities
Fractures
Breccias
ESF 27+84
Opal
Top
Resin
Calcite
Base
Tuff
A
ESF 48+11
Calcite
D
ECRB 12+90
Base
Tuff
Top
Top
Resin
Calcite
Base
G
Resin
Top
ESF 28+81
Calcite
Base
B
ESF 04+44
Resin
Top
C
Cdy
Base
Resin
Tuff
E
ESF 74+19
Top
Resin
Base
Tuff
H
ECRB 08+51
Top
Resin
C
Base
Tuff
C
ESF 28+80
Opal
Resin
Calcite
Top
Tuff
Cdy
Tuff
Base
F
I
Resin
Tuff
Calcite
Tuff
ESF 01+62.3

Figure 3

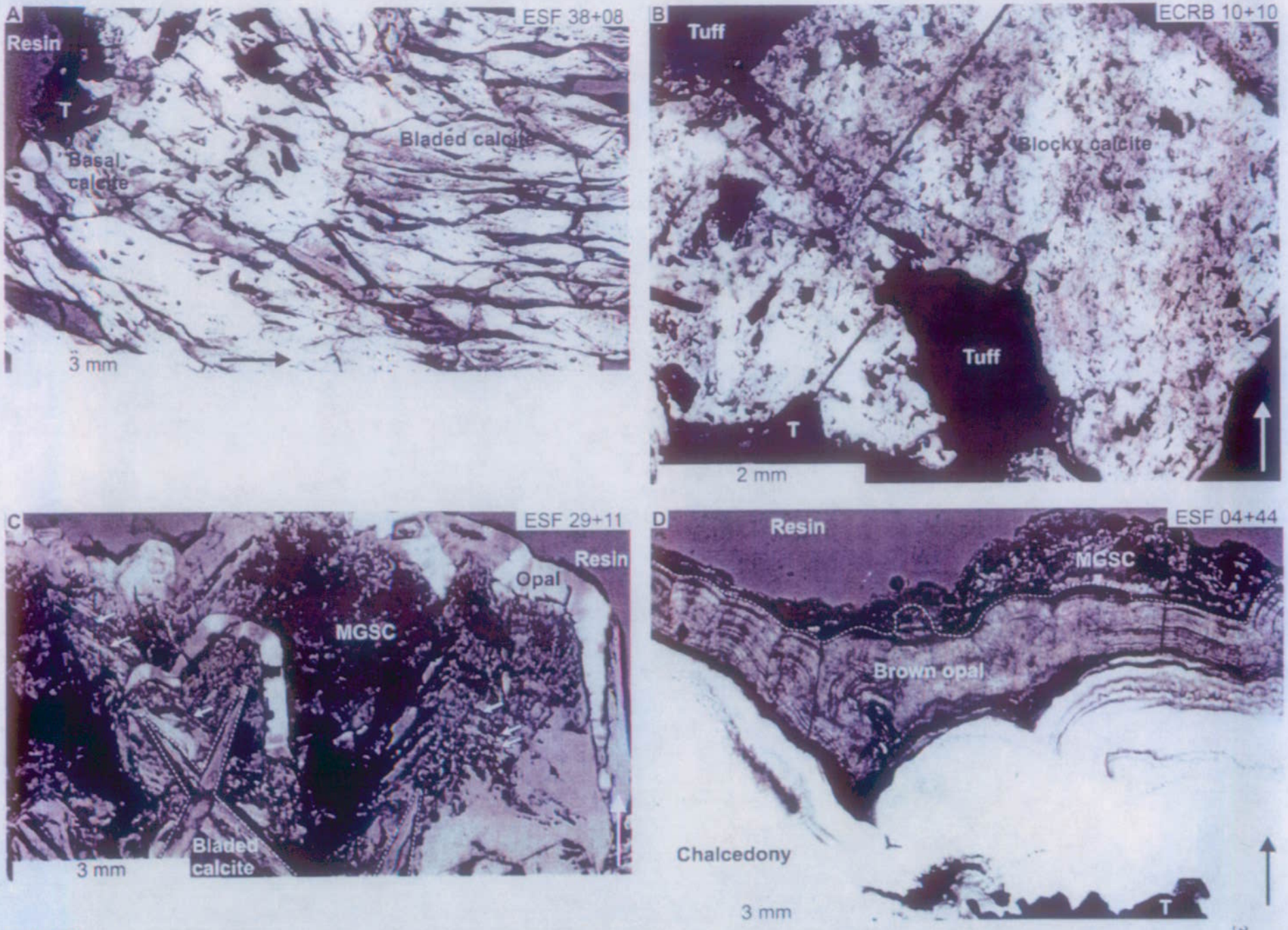
A
ESF 38+08
Resin
T
Basal calcite
Bladed calcite
3 mm
B
ECRB 10+10
Tuff
Blocky calcite
Tuff
T
2 mm
C
ESF 29+11
Resin
Opal
MGSC
Bladed calcite
3 mm
D
ESF 04+44
Resin
MGSC
Brown opal
Chalcedony
T
3 mm

Figure 4

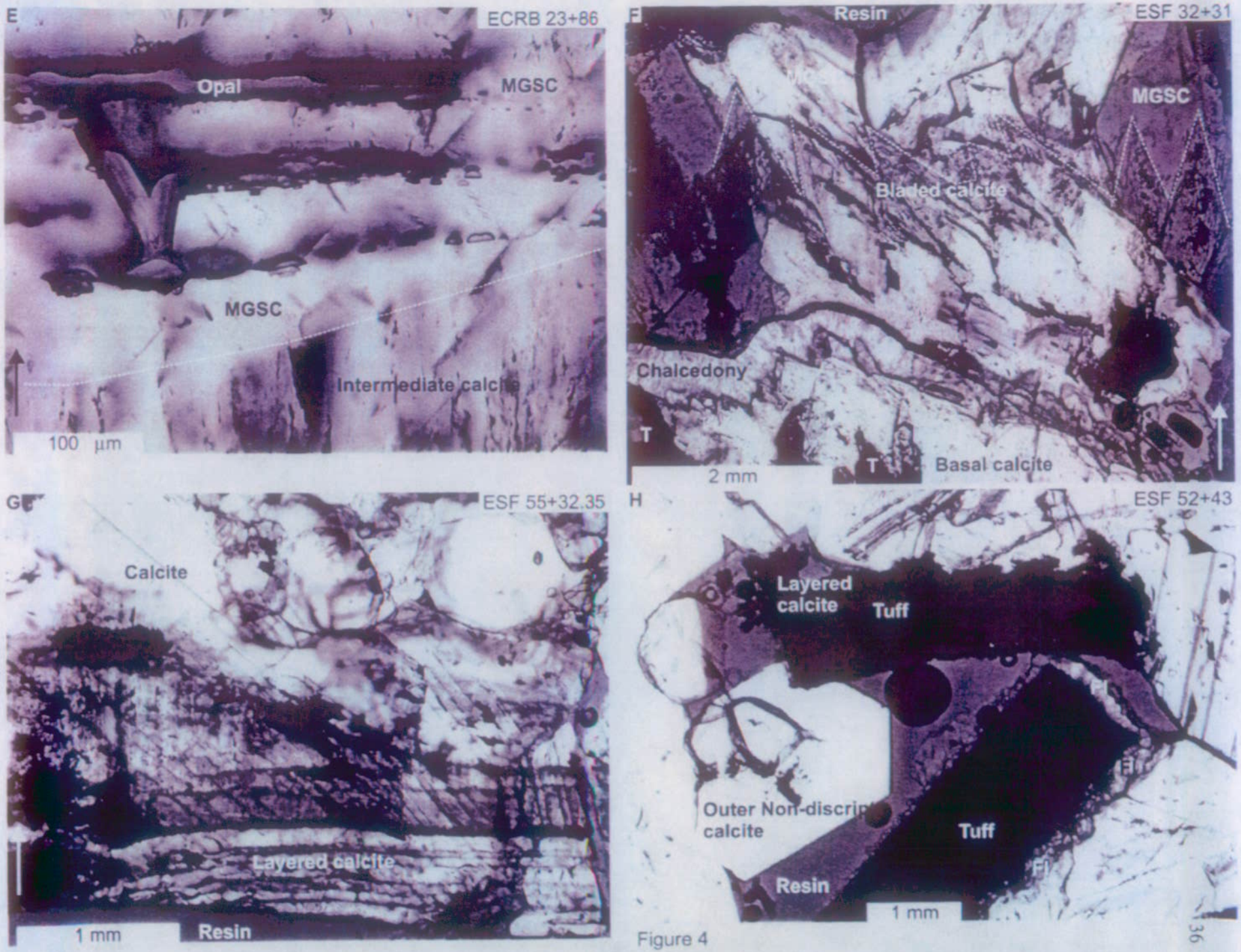
E
ECRB 23+86
Opal
MGSC
MGSC
Intermediate calcite
100 µm
F
Resin
ESF 32+31
MGSC
Bladed calcite
Chalcedony
T
T
Basal calcite
2 mm
G
ESF 55+32.35
Calcite
Layered calcite
1 mm
Resin
H
ESF 52+43
Layered calcite
Tuff
Outer Non-discrim
calcite
Tuff
Resin
1 mm

Figure 4

Figure 4

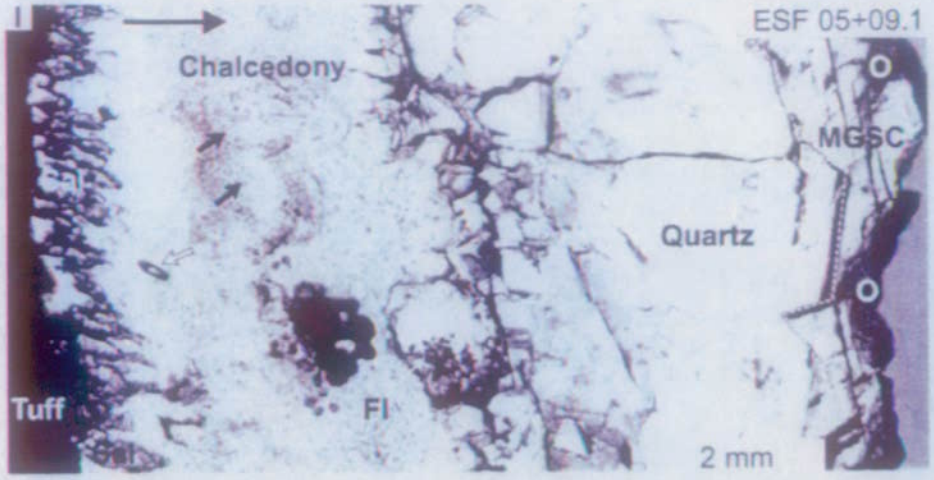
I
ESF 05+09.1
Chalcedony
MGSC
Quartz
Tuff
Fl
2 mm

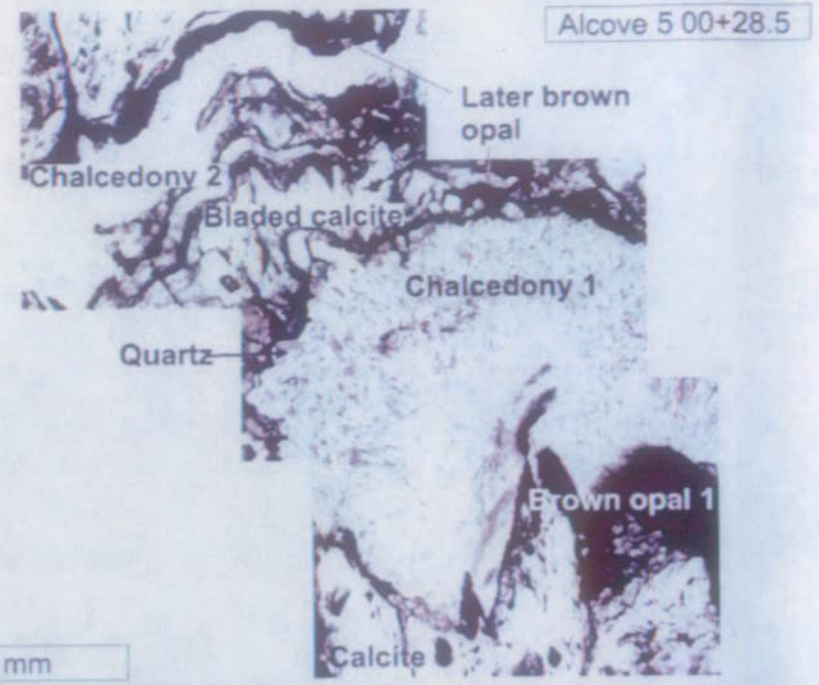
J
Alcove 5 00+28.5
Later brown opal
Chalcedony 2
Bladed calcite
Chalcedony 1
Quartz
Brown opal 1
Calcite
2 mm

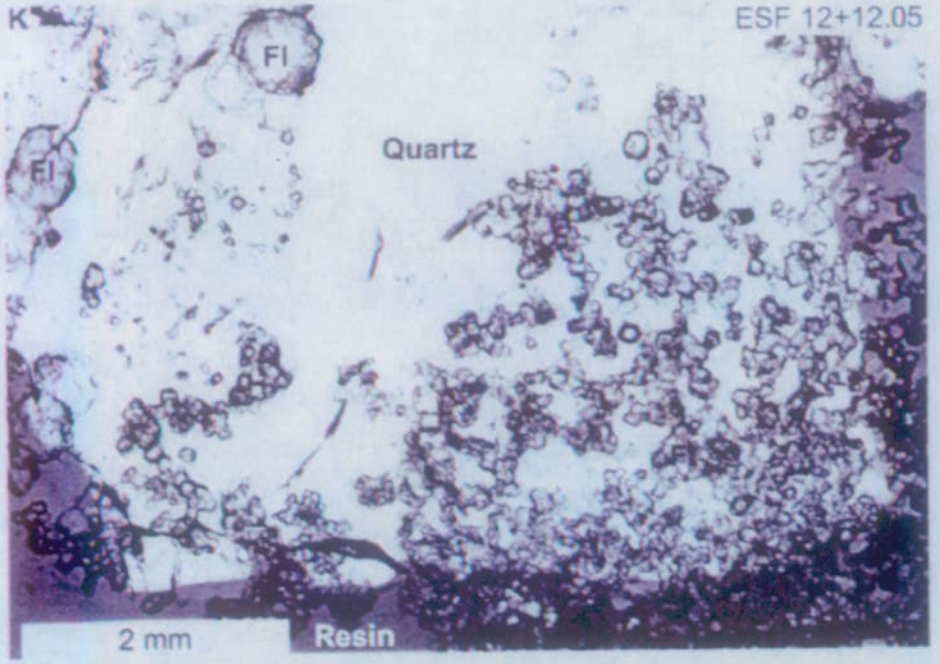
K
ESF 12+12.05
Fl
Fl
Quartz
2 mm
Resin

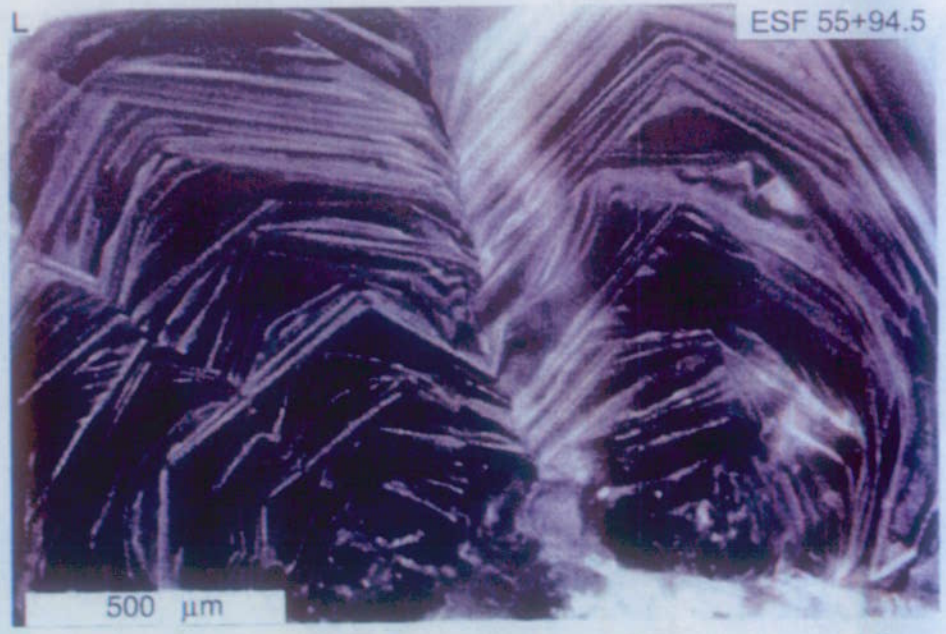
L
ESF 55+94.5
500 µm

Figure 5

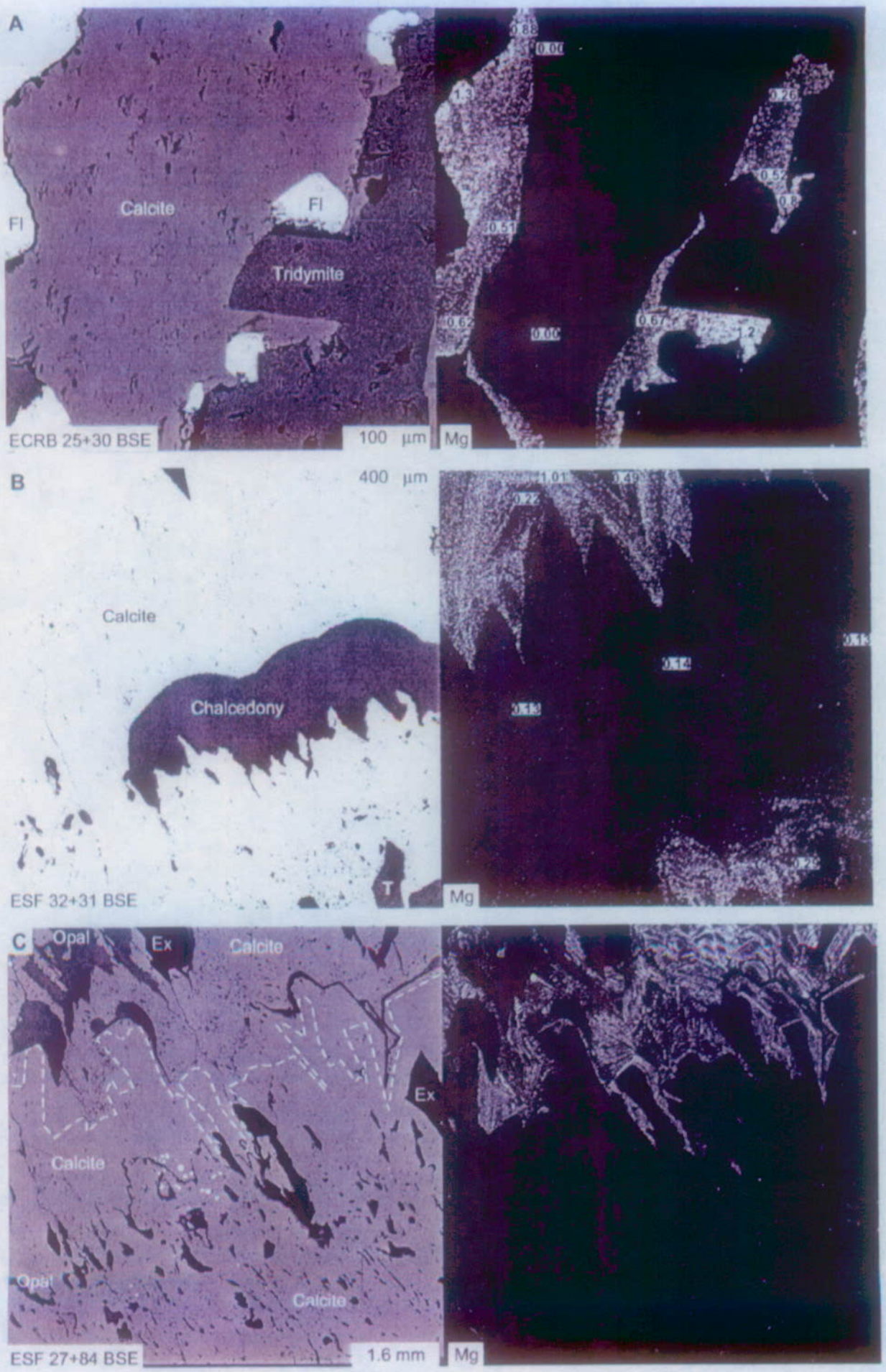
A
Calcite
Fl
Fl
Tridymite
ECRB 25+30 BSE
100 µm
Mg
B
400 µm
Calcite
Chalcedony
T
ESF 32+31 BSE
Mg
C
Opal
Ex
Calcite
Ex
Calcite
Opal
Calcite
ESF 27+84 BSE
1.6 mm
Mg

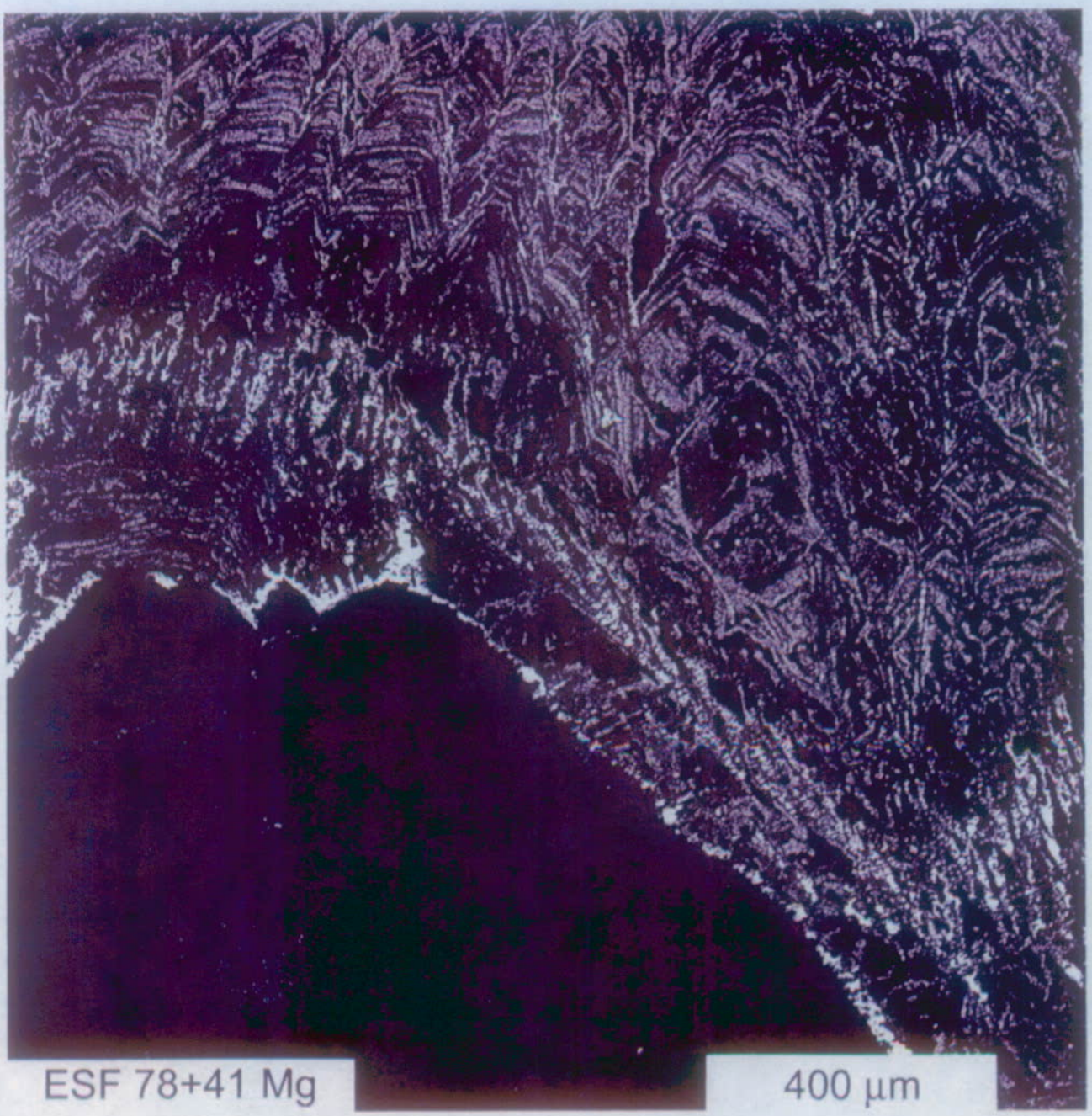

Figure 6

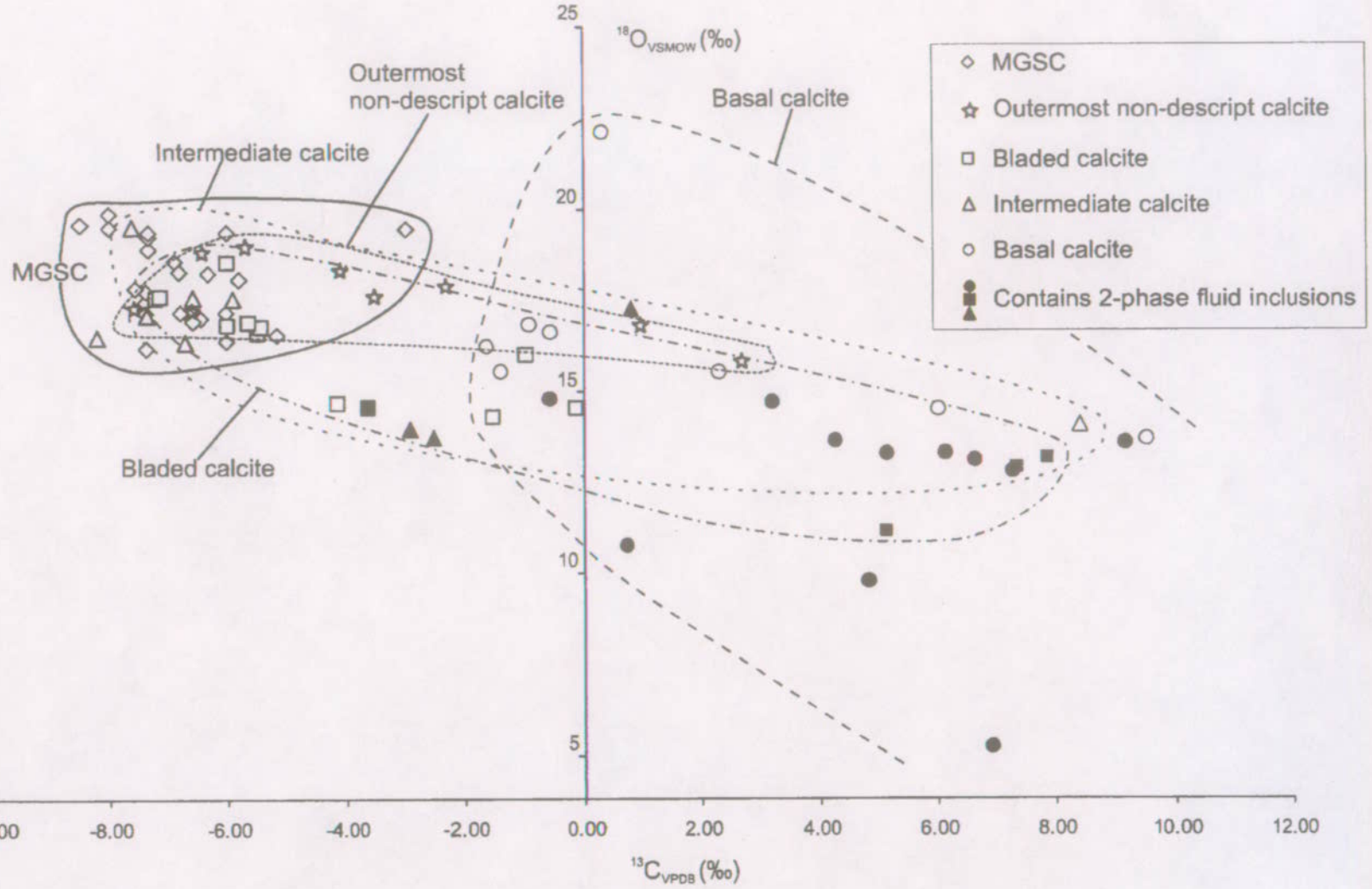
25
20
15
10
5
$^{18}O_{VSMOW}$ (‰)
Outermost
non-descript calcite
Basal calcite
Intermediate calcite
MGSC
Bladed calcite
MGSC
Outermost non-descript calcite
Bladed calcite
Intermediate calcite
Basal calcite
Contains 2-phase fluid inclusions
-10.00
-8.00
-6.00
-4.00
-2.00
0.00
2.00
4.00
6.00
8.00
10.00
12.00
$^{13}C_{VPDB}$ (‰)

Figure 7

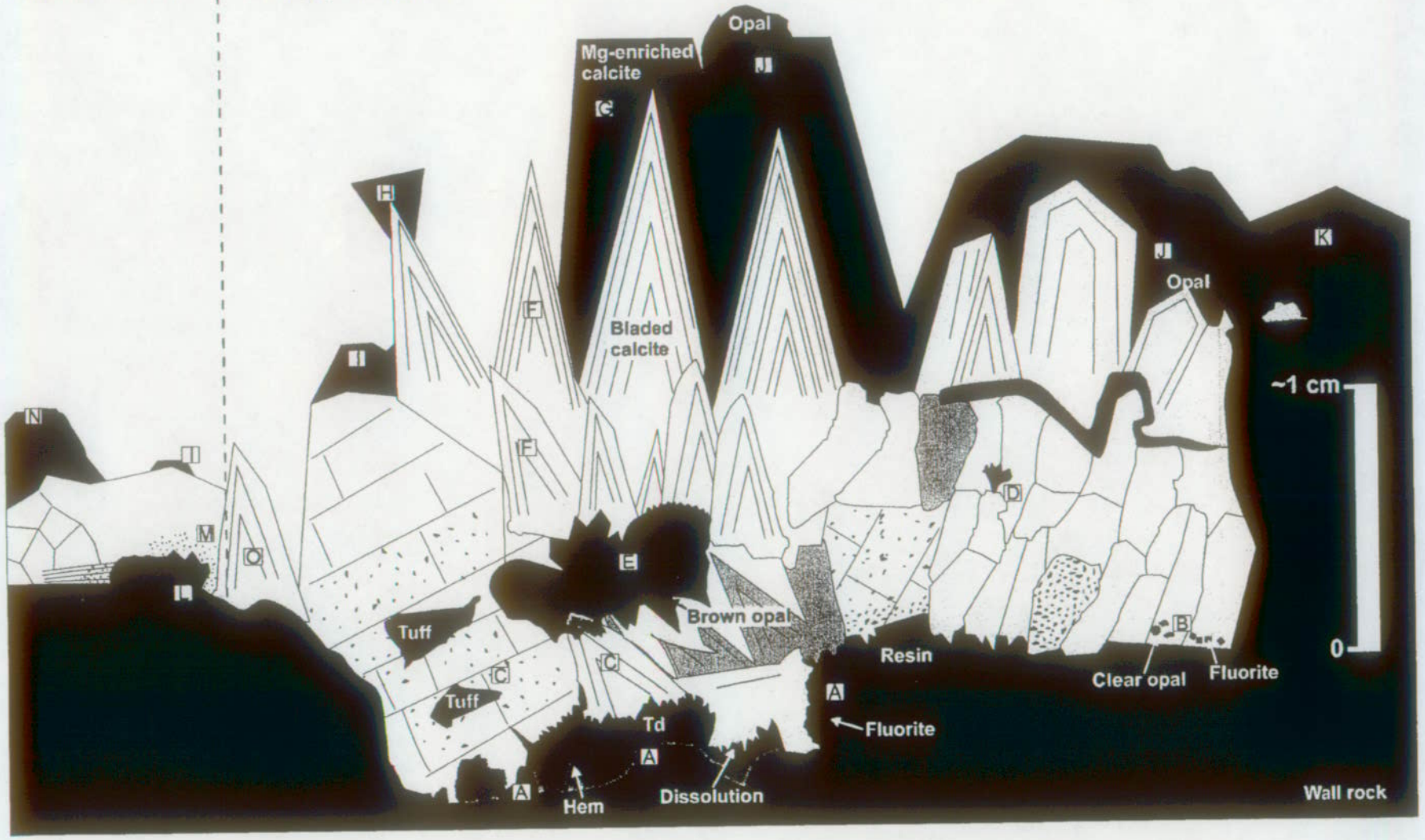
Fracture / Breccia
Lithophysal Cavities
Opal
Mg-enriched calcite
G
N
H
F
Bladed calcite
I
J
Opal
K
~1 cm
0
N
I
F
M
O
E
D
L
Brown opal
B
Tuff
C
C
Resin
Clear opal
Fluorite
Tuff
A
Td
Fluorite
A
A
Hem
Dissolution
Wall rock

Figure 8

Table 1. C and O isotope data for calcite samples and calibration standards

Sample	Sample Split	Sample description	$\delta^{13}C$ (‰)	$\delta^{18}O$ (‰)
ECRB 04+87	B17	Basal calcite	-1.4	15.5
ECRB 04+87	B16	Bladed calcite	-4.2	14.7
ECRB 04+87	A2	Bladed calcite	-5.5	16.6
ECRB 04+87	A3	MGSC	-7.3	17.4
ECRB 12+90*	A1	Basal calcite	9.1	13.6
ECRB 12+90	B11	Bladed calcite	-1.0	16.0
ECRB 12+90	A2	Intermediate calcite	-6.6	17.6
ECRB 12+90	A3	MGSC	-6.4	17.0
ECRB 12+90	B12	MGSC	-6.6	16.9
ECRB 14+69	A1	Basal calcite	3.9	15.3
ECRB 14+69	A2	Outer basal calcite	-1.6	16.2
ECRB 14+69	A4	MGSC	-6.6	17.1
ESF 01+62.3*	A1	Basal calcite	0.7	10.9
ESF 01+62.3*	A2	Intermediate calcite	0.8	17.1
ESF 01+62.3	A3	Outer non-descript calcite	-4.1	18.3
ESF 01+62.3	A4	Outer non-descript calcite	-5.7	19.0
ESF 04+73.4*	B10	Basal calcite	6.8	5.2
ESF 04+73.4	A3	MGSC	-6.0	19.4
ESF 05+09.1	A1	outer sparry calcite	-3.0	19.5
ESF 13+19	A2	outer clear calcite above fluorite and quartz	-2.3	17.9
ESF 14+75.8*	A4	Basal calcite	4.8	9.9
ESF 27+84*	B6	Basal calcite	5.1	13.3
ESF27+84*	C17	Central basal calcite	-0.6	14.8
ESF 27+84	B8	Intermediate calcite	-6.7	16.3
ESF 27+84	A1	Intermediate calcite	-8.2	16.4
ESF 27+84	A2	MGSC	-7.3	16.2
ESF 27+84	A3	MGSC	-7.3	17.1
AL#5 00+28.5*	C10	Basal calcite	7.2	12.9
AL#5 00+28.5*	C11	Outer basal calcite	4.2	13.7
AL#5 00+28.5*	C12	Intermediate calcite	-2.5	13.4
AL#5 00+28.5*	C15	Intermediate calcite	-2.9	13.7
AL#5 00+28.5*	C16	Bladed calcite	-3.6	14.4
ESF 28+81*	A3	Bladed calcite	7.3	13.0
ESF 28+81*	A2	Bladed calcite	5.1	11.2
ESF 28+81*	A1	Bladed calcite	7.9	13.2
ESF 28+81	A4	Outer bladed calcite	-0.1	14.4
ESF 28+81	A5	Outer bladed calcite	-1.5	14.2
ESF 29+11	C8	MGSC	-5.2	16.5
ESF 29+11	C9	MGSC	-6.8	17.2
ESF 32+31	C6	Basal calcite	9.5	13.8
ESF 32+31	C7	MGSC	-6.0	17.2
ESF 34+86.5	B9	Basal calcite	6.0	14.5

Table 1. Continued.

Sample	Sample Split	Sample description	$\delta^{13}C$ (‰)	$\delta^{18}O$ (‰)
ESF 34+86.5	A5	Bladed calcite	-5.4	16.7
ESF 34+86.5	A6	Bladed calcite	-6.0	16.9
ESF 34+86.5	A3	MGSC	-6.0	16.4
ESF 34+86.5	A7	Bladed calcite	-5.6	16.9
ESF 43+83.5	A2	Basal calcite	-0.6	16.6
ESF 43+83.5	A3	Intermediate calcite	-5.9	17.5
ESF 43+83.5	A4	Outer non-descript calcite	-7.5	17.3
ESF 46+79*	B13	Basal calcite	3.2	14.9
ESF 46+79	B14	Basal calcite	2.3	15.4
ESF 46+79	B15	Outer non-descript calcite	-3.5	17.6
ESF 48+11	A1	Basal calcite	-0.9	16.8
ESF 48+11	A2	Outer non-descript calcite	-6.6	17.2
ESF 52+65.2	A3	Outermost non-descript calcite	2.7	15.7
ESF 52+65.2	A2	Outermost non-descript calcite	1.0	16.8
ESF 52+65.2	A1	Outer non-descript calcite	-6.4	18.8
ESF 60+52.5	A3	MGSC	-6.3	18.2
ESF 60+52.5	A2	MGSC	-6.9	18.6
ESF 64+95*	E2	Basal calcite	6.1	13.5
ESF 64+95*	E3	Basal calcite	6.6	13.2
ESF 64+95	E4	Bladed calcite	-7.2	17.5
ESF 64+95	E5	MGSC	-7.3	17.8
ESF 64+95	E1	MGSC	-7.5	17.8
ESF 64+95	A2	Bladed calcite	-7.1	17.6
ESF 67+81	C4	Basal calcite	0.3	22.1
ESF 67+81	C5	MGSC	-6.8	18.3
ESF 72+25	C13	Bladed calcite	-6.0	18.5
ESF 72+25	C14	MGSC	-5.8	18.1
ESF 77+03	B18	Intermediate calcite	8.4	14.1
ESF 76+59.5	C2	Intermediate calcite	-7.6	19.5
ESF 76+59.5	C3	MGSC	-7.3	18.9
ESF 78+05.2	B1	MGSC	-7.3	19.2
ESF 78+05.2	B5	MGSC	-7.3	19.4
ESF 78+05.2	B4	MGSC	-8.0	19.5
ESF 78+05.2	B2	MGSC	-8.0	19.9
ESF 78+05.2	B3	MGSC	-8.5	19.6
Standards				
NBS 18		Carbonatite (n=7)	-5.0 to -4.9	7.0 to 7.2
NBS 19		Marble (n=7)	1.9 to 2.0	28.6 to 28.8
NBS 20		Solenhofen Lst (n=3)	-1.1 to -1.0	26.6 to 26.7
LIPS		A1 (n=1)	1.1	24.9
YULE		Marble (n=1)	-2.7	23.9

* Sampled calcite contained 2-phase fluid inclusions.